

WISCONSIN HIGHWAY RESEARCH PROGRAM #0092-00-12

**EQUIVALENCY OF CRUSHED ROCK WITH INDUSTRIAL  
BY-PRODUCTS AND GEOSYNTHETIC-REINFORCED  
AGGREGATES USED FOR WORKING PLATFORMS  
DURING PAVEMENT CONSTRUCTION**

**A FINAL REPORT on the WHRP Project  
“Equivalency of Subgrade Reinforcement Methods”**

Principal Investigators: Craig H. Benson and Tuncer B. Edil

Graduate Research Assistants: Burak F. Tanyu and  
Woon-Hyung Kim

Geo Engineering Program  
Department of Civil and Environmental Engineering  
University of Wisconsin-Madison

SUBMITTED TO THE WISCONSIN DEPARTMENT OF  
TRANSPORTATION

October 31, 2005

## **ACKNOWLEDGEMENT**

Financial support for the study described in this paper was provided by the Wisconsin Department of Transportation (WisDOT) through the Wisconsin Highway Research Program (WHRP). Alliant Energy Corporation supplied the bottom ash, Grede Foundries Inc. supplied the foundry sand and foundry slag, and Yahara Materials supplied the Grade 2 granular backfill. Tenax Corporation and Amoco Fabrics and Fibers Co. supplied the geosynthetics. The LSME experiments were conducted in the University of Wisconsin Structures and Materials Testing Laboratory (SMTL). Professor Steven Cramer (Director of SMTL) and Mr. William Lang (Manager of SMTL) provided valuable assistance during the LSME tests. The RWD tests were conducted by Professor James A. Crovetti of Marquette University. The conclusions and recommendations in this report are solely those of the authors, and do not necessarily reflect the opinions or policies of WisDOT, WHRP, the material suppliers, or others who provided assistance during the study. Endorsement by persons other than the authors is not implied and should not be assumed.

## **DISCLAIMER**

This research was funded through the Wisconsin Highway Research Program by the Wisconsin Department of Transportation and the Federal Highway Administration under Project # 0092-00-12. The contents of this report reflect the views of the authors who are responsible for the facts and accuracy of the data resented herein. The contents do no necessarily reflect the official views of the Wisconsin Department of Transportation or the Federal Highway Administration at the time of publication.

This document is disseminated under the sponsorship of the Department of Transportation in the interest of information exchange. The United State Government assumes no liability for its contents or use thereof. This report does not constitute a standard, specification or regulation.

The United States Government does not endorse products or manufacturers. Trade and manufacturers' names appear in this report only because they are considered essential to the object of the document.

## Technical Report Documentation Page

|  |  |  |                                 |
|--|--|--|---------------------------------|
| 1. Report No. 0092-00-12   | 2. Government Accession No                               | 3. Recipient's Catalog No  |                                 |
| 4. Title and Subtitle<br><br>Equivalency of Subgrade Reinforcement Methods   |  | 5. Report Date   | 6. Performing Organization Code |
| 7. Authors<br>Craig H. Benson, Tuncer B. Edil, Burak F. Tanyu, and Woon-Hyung Kim  |  | 8. Performing Organization Report No.  |                                 |
| 9. Performing Organization Name and Address<br>Department of Civil and Environmental Engineering<br>University of Wisconsin-Madison<br>1415 Engineering Drive<br>Madison, WI 53706   |  | 10. Work Unit No. (TR AIS)   | 11. Contract or Grant No.       |
| 12. Sponsoring Agency Name and Address<br>Wisconsin Department of Transportation<br>4802 Sheboygan Avenue<br>Madison, WI 73707-7965  |  | 13. Type of Report and Period Covered  | 14. Sponsoring Agency Code      |
| 15. Supplementary Notes  |  |  |                                 |
| <p><b>16. Abstract</b></p> <p>A study was conducted to define an equivalency criterion for five materials used for working platforms during pavement construction on a poor subgrade: conventional crushed rock (referred to as "breaker run") and four alternatives (i.e. Grade 2 granular backfill (referred to as "Grade 2"), foundry slag, bottom ash, and foundry sand). Total deflection data for the equivalency assessment were obtained from a large-scale model experiment (LSME) simulating a prototype-scale pavement structure and in the field using a rolling wheel deflectometer (RWD). Design charts were developed for selecting the equivalent thickness of alternative working platform materials so that the alternative provides equal deflection as a layer of breaker run.</p> <p>Another phase of the study was conducted to determine the equivalency of geosynthetic-reinforced aggregate working platforms in providing support during pavement construction over soft subgrade. Four reinforcing geosynthetics (a geogrid, a woven geotextile, a non-woven geotextile, and drainage geocomposite) incorporated into two granular materials: Grade 2 and breaker run were used in this study. Design charts were developed for selecting the equivalent thickness of an alternative geosynthetic-reinforced working platform material so that the alternative provides equal deflection as a layer of breaker run.</p> |  |  |                                 |
| <p><b>17. Key Words</b><br/>working platform, industrial by-product, geosynthetic, pavement construction, subgrade reinforcement, gravel, crushed rock, equivalency, sustainable development, beneficial reuse</p>   |  | <p><b>18. Distribution Statement</b><br/>No restriction. This document is available to the public through the National Technical Information Service<br/>5285 Port Royal Road<br/>Springfield VA 22161</p> |                                 |
| 19. Security Classif.(of this report)<br><br>Unclassified  | 19. Security Classif. (of this page)<br><br>Unclassified | 20. No. of Pages   | 21. Price                       |

## EXECUTIVE SUMMARY

The objective of this study was to develop a method for selecting the thickness of four alternative materials used in lieu of “breaker run” crushed rock as a working platform for highway construction on very soft subgrade. Breaker run is commonly used for working platforms, and thus was selected as the reference material. Three industrial byproducts (bottom ash, foundry slag, and foundry sand) and a granular backfill were used as alternative materials. A working platform of alternative material was considered equivalent to that with breaker run if the total deflection of the alternative material was equal to the total deflection of breaker run under the same construction loading.

Large-scale model experiments were conducted on each of the working platform materials to define the relationship between total deflection and working platform thickness for a typical construction loading (1000 trips of a loaded 4-axle dump truck). A simulated very soft subgrade was used in the experiments so that the findings could be used conservatively for most soft subgrade applications. Results of the large-scale tests were used to develop design charts relating the thickness of an alternative material required to achieve the same total deflection as a working platform of breaker run. The method for selecting equivalent thicknesses was checked with field data from a rolling weight deflectometer (RWD) test and an unpaved road design method from the literature. Both comparisons were favorable.

One of the design charts relates thickness of the alternative material to CBR. This chart is conceptual because the curves have not yet been validated with additional data. Nevertheless, the trends are consistent in that a thinner working platform is required when the alternative material has higher CBR, and a thicker working platform is needed when the required deflection is smaller. The chart also shows that very thick working platforms may be required for alternative materials having a  $CBR < 20$ . Thus, some alternative materials may not be economical substitutes for working platforms constructed with crushed rock in some projects.

Another phase of the study was conducted to determine the equivalency of geosynthetic-reinforced aggregate working platforms in providing support during pavement construction over soft subgrade. Large-scale experiments were conducted on working platforms of crushed rock (breaker run stone) or gravel (Grade 2 granular backfill) overlying a simulated soft subgrade. Tests were conducted with and without geosynthetic reinforcement to evaluate how the required thickness of the working platform is affected by the presence of reinforcement. Four different geosynthetics were used (geogrid, woven geotextile, nonwoven geotextile, and drainage composite), each having different in situ extensibility.

Working platforms reinforced by geosynthetics accumulated deformation at a slower rate than unreinforced working platforms, and in most cases deformation of the geosynthetic-reinforced working platforms nearly ceased after 200 loading cycles. As a result, total deflections were always smaller (about a factor of two) for reinforced working platforms relative to unreinforced working platforms. Smaller deflections were also associated working platforms that were thicker or reinforced with less extensible geosynthetics.

Thicknesses for equivalent working platforms reinforced with various types of geosynthetics were developed for a range of target total deflections and related to a measure of in situ extensibility characterized by an interaction modulus obtained from a pullout test. The equivalent thickness of geosynthetic reinforced material diminished approximately linearly with increasing logarithm of the interaction modulus (decreasing in situ extensibility of the geosynthetic). Moreover, the thickness ratio is lower when the target total deflection is smaller, indicating that the benefits of geosynthetic reinforcement are greater when the target deflection is lower.

The relationships in the equivalency table are based on the LSME tests for the specific geosynthetics used in this study and for a very soft subgrade condition. Therefore, the generality of the findings is not implied. However, this methodology, including the interaction modulus, can be considered in determining equivalency of other reinforcement-aggregate platforms.

## TABLE OF CONTENTS

|   |      |
|---|------|
| ACKNOWLEDGMENTS .....   | i    |
| DISCLAIMER.....   | ii   |
| TECHNICAL REPORT DOCUMENTATION PAGE .....   | iii  |
| EXECUTIVE SUMMARY .....   | iv   |
| TABLE OF CONTENTS.....  | vi   |
| LIST OF TABLES.....   | viii |
| LIST OF FIGURES .....   | ix   |
| CHAPTER ONE: EQUIVALENCY OF CRUSHED ROCK AND THREE<br>INDUSTRIAL BY-PRODUCTS USED FOR WORKING PLATFORMS DURING<br>PAVEMENT CONSTRUCTION ..... | 1    |
| 1.1 INTRODUCTION .....  | 1    |
| 1.2 MATERIALS .....   | 3    |
| 1.3 LARGE-SCALE TESTS .....   | 9    |
| 1.3.1 Pavement Profile.....   | 9    |
| 1.3.2 Loads and Deflections.....  | 12   |
| 1.4 FIELD METHODS.....  | 13   |
| 1.5 RESULTS AND ANALYSIS .....  | 15   |
| 1.5.1 Total Deflection Basins .....   | 15   |
| 1.5.2 Relationship Between Thickness and Maximum Total<br>Deflection .....  | 22   |
| 1.5.3 Comparison of Total Deflections from RWD and LSME.....  | 25   |
| 1.5.4 Comparison with Unpaved Road Design Methods.....  | 28   |
| 1.6 EQUIVALENCY SELECTION METHOD.....   | 30   |
| 1.7 CONSTRUCTION ISSUES.....  | 34   |

|      |   |    |
|------|---|----|
| 1.8  | SUMMARY AND CONCLUSIONS.....  | 34 |
| 1.9  | GUIDELINES FOR USING INDUSTRIAL BYPRODUCTS AS<br>WORKING PLATFORM.....  | 37 |
| 2.0  | REFERENCES .....  | 38 |
| <br> |   |    |
|      | CHAPTER TWO: EQUIVALENCY OF GEOSYNTHETIC-REINFORCED<br>AGGREGATE MATERIALS USED FOR WORKING PLATFORMS DURING<br>PAVEMENT CONSTRUCTION ..... | 42 |
| 2.1  | INTRODUCTION .....  | 42 |
| 2.2  | BACKGROUND .....  | 43 |
| 2.3  | MATERIALS .....   | 46 |
| 2.4  | PULLOUT TESTS.....  | 52 |
| 2.5  | LARGE-SCALE MODEL EXPERIMENT (LSME).....  | 53 |
|      | 2.5.1 Subgrade and Pavement Profile .....   | 54 |
|      | 2.5.2 Loads and Deflections.....  | 57 |
|      | 2.5.3 Instrumentation .....   | 58 |
| 2.6  | RESULTS AND ANALYSIS .....  | 59 |
|      | 2.6.1 Pullout Tests .....   | 59 |
|      | 2.6.2 LSME Tests .....  | 61 |
|      | 2.6.2.1 Total Deflection Basins.....  | 61 |
|      | 2.6.2.2 Effect of Layer Thickness on The Total Deflection<br>Basins.....  | 62 |
|      | 2.6.2.3 Effect of Geosynthetic Type on The Total Deflection<br>Basins.....  | 65 |
|      | 2.6.3 Permanent Deformation Analysis.....   | 70 |
|      | 2.6.4 Relationship Between Platform Thickness and Total<br>Deflection .....   | 73 |
|      | 2.6.5 Equivalency Chart.....  | 77 |
| 2.7  | PRACTICAL IMPLICATIONS .....  | 80 |
| 2.8  | CONSTRUCTION ISSUES .....   | 82 |
| 2.9  | SUMMARY AND CONCLUSIONS.....  | 83 |
| 3.0  | REFERENCES .....  | 82 |

## LIST OF TABLES

|            |  |    |
|------------|--|----|
| Table 1.1. | Properties of working platform materials .....   | 6  |
| Table 1.2. | Maximum total deflections directly underneath loading plate for all tests conducted in LSME along with parameters of Eq. 1.1.....  | 18 |
| Table 1.3. | Total deflections obtained from RWD and estimated with Eq. 1.1 using parameters fitted to data from the LSME tests. Number of RWD measurements noted in parentheses .....              | 27 |
| Table 2.1. | Properties of Grade 2 and breaker run in LSME tests.....   | 48 |
| Table 2.2. | Properties of geosynthetics used in LSME tests .....   | 50 |
| Table 2.3. | Permanent deformation parameters with and without geosynthetic reinforcements .....  | 72 |
| Table 2.4. | Geosynthetic-Reinforced Aggregate Platform Thickness (h in meters) Required to Achieve the Total Deflection ( $\delta_t$ in millimeters) Limited to 12.5 mm, 25.0 mm, and 37.5 mm..... | 75 |

## LIST OF FIGURES

|            |  |    |
|------------|--|----|
| Fig. 1.1.  | Acceptable range of the particle size distribution for Grade 2 according to WisDOT (1996) along with particle size distribution of Grade 2 used in this study (a) and particle size distributions of working platform materials used in this study (b) .....   | 7  |
| Fig. 1.2.  | Compaction curves and water content-dry unit weight data from field sections and LSME: bottom ash (a), foundry slag (b), Grade 2 (c) and foundry sand (d).....   | 8  |
| Fig. 1.3.  | Schematic cross section of Large-Scale Model Experiment (LSME) ..  | 10 |
| Fig. 1.4.  | Pavement profiles and properties of subgrade and working Platforms at STH 60 field site .....  | 14 |
| Fig. 1.5.  | Cumulative total deflection under the loading plate of the LSME as a function of number of load cycles for working platforms constructed with Grade 2 having a thickness (h) of 0.31 and 0.46 m.....   | 16 |
| Fig. 1.6.  | Deflection basins for working platforms: (a) basins for breaker run and bottom ash showing the effect of thickness and (b) basins for all materials when the thickness of the working platform is 0.46 m (b) .....   | 19 |
| Fig. 1.7.  | Deflection basins for foundry sand prepared at optimum water content (16%), 4% dry of optimum water content (12%), and 7% wet of optimum water content (23%). The test at a water content of 23% was stopped at 40 loading cycles because the deflection was so large that the stroke limit of the actuator was reached..... | 21 |
| Fig. 1.8.  | Relationship between layer thickness and total deflection for working platforms constructed with bottom ash .....  | 23 |
| Fig. 1.9.  | Total deflections at the field site measured using the RWD.....  | 26 |
| Fig. 1.10. | Design chart relating thickness of each alternative material to thickness of breaker run.....  | 31 |
| Fig. 1.11. | Design chart relating ratio of thickness of working platform of an alternative material ( $h_a$ ) to the thickness of breaker run ( $h_b$ ) required to limit total deflections to 12, 25, and 50 mm as a function of normalized CBR (CBR of alternative material $\div$ CBR of breaker run) .....                           | 33 |

|            |  |    |
|------------|--|----|
| Fig. 2.1.  | Particle-size distributions of Grade 2 and breaker run based on mechanical sieve analysis.....   | 47 |
| Fig. 2.2.  | Comparison of wide width strength (ASTM D 4595) for geosynthetics used in the LSME tests: (a) machine direction and (b) cross-machine direction .....  | 51 |
| Fig. 2.3.  | Schematic cross section of large-scale model experiment (LSME) ....  | 55 |
| Fig. 2.4.  | Results of pullout test showing the relationship between force per unit width and displacement for: (a) geogrid; (b) woven geotextile; (c) non-woven geotextile; and (d) drainage geocomposite .....   | 60 |
| Fig. 2.5.  | Cumulative total deflection ( $\delta_t$ ) under the loading plate of the LSME as a function of number of load cycles for aggregate platforms having a thickness (h) of 0.30 m or 0.46 m. Geosynthetic-reinforced platforms are constructed only with Grade 2.....   | 63 |
| Fig. 2.6.  | Effect of layer thickness on the total deflection for geogrid and non-woven geotextile-reinforced platforms in the LSME: (a) deflection basins after 1,000 load cycles and (b) gauge strain and telltale movement in the geosynthetic at the edge of the loading plate as a function of number of load cycles .....  | 64 |
| Fig. 2.7.  | Effect of geosynthetic type on the total deflection for Grade 2 platforms reinforced with geosynthetics when the platform thickness is 0.30 m (i.e., h = 0.30 m): (a) deflection basins after 1,000 load cycles in the LSME and (b) gauge strain and telltale movement in the geosynthetic at the edge of the loading plate as a function of number of load cycles ..... | 67 |
| Fig. 2.8.  | Comparison of moduli from wide width tensile test and pullout test for geosynthetics used in the LSME .....  | 68 |
| Fig. 2.9.  | Accumulation of plastic strain during the LSME test of Grade 2 gravel with and without geosynthetic reinforcement (h = working platform thickness).....  | 71 |
| Fig. 2.10. | Comparison of normalized equivalency thickness between the unreinforced breaker run and the geosynthetic-reinforced Grade 2 gravel tested based on the total deflections being limited to 12.5, 25.0, and 37.5 millimeters.....  | 76 |

Fig. 2.11. Equivalency chart relating thickness of each geosynthetic-reinforced platform to the thickness of the breaker run..... 78

Fig. 2.12. Relationship between normalized equivalency thicknesses and the interaction modulus from the pullout test for various geosynthetics ..... 81

## **CHAPTER ONE**

# **EQUIVALENCY OF CRUSHED ROCK AND THREE INDUSTRIAL BY-PRODUCTS USED FOR WORKING PLATFORMS DURING PAVEMENT CONSTRUCTION**

### **1.1 INTRODUCTION**

Deformation of soft fine-grained subgrade soils often is problematic during construction of pavements as well as under regular vehicular traffic loads. Subgrade rutting during construction due to heavy truck loads can impede construction equipment and complicate placement of subbase and base layers. After construction, accumulation of plastic shear strain and consolidation of the subgrade can result in rutting of the asphalt surface under repeated traffic loading (Shackel 1973, Monismith 1976, Wood 1982, Huang 1993, Li and Selig 1996). Previous studies on this issue have focused primarily on estimating the cumulative deflection of subgrade under long-term in-service loading conditions (Monismith et al. 1975, Chou 1976, Claussen et al. 1977, Shook et al. 1982, Finn et al. 1986, Thompson and Nauman 1993, Li and Selig 1996,). Less attention has been placed on deformation of soft subgrade during construction, although soft subgrade soils have long been known to provide inadequate support for construction truck traffic. A literature survey showed that there is limited published literature regarding rutting and yielding of subgrade during construction. In Wisconsin, construction on soft subgrade soils has been identified as a major issue affecting cost and scheduling due to problems associated with construction delays, change orders, additional costs, and contract administration problems (WisDOT 1997).

Traditional practice in Wisconsin, as well as in other Midwestern states, has been to undercut the soft subgrade and replace it with a layer of “select” granular material (WisDOT 2003). The most common select material is a broadly graded crushed rock with large particles referred to as “breaker run” (WisDOT 1997). The high cost of select materials such as breaker run has led to keen interest in alternative materials. Granular industrial by-products are of particular interest because they can be obtained at low cost while fostering sustainable development.

The objective of this study was to determine the thickness of working platforms constructed with four alternative materials (three granular industrial by-products and a gravel) that would result in the same cumulative total deflection as a layer of breaker run under typical construction loadings. The study was directed to respond to needs in Wisconsin, but the findings are applicable to other locations where breaker run is used. Alternative working platforms that provide equal deflection as a working platform to that of breaker run are referred to herein as being “equivalent.” This definition of equivalency applies only to the cumulative total deflection during construction; therefore, the emphasis is on short-term response. Other issues (e.g. service life expectancy, drainage, weathering, etc.) under in-service loading conditions also need to be considered for long-term pavement performance, but are not addressed herein.

## 1.2 MATERIALS

The Wisconsin Department of Transportation has identified eight select material alternatives for stabilization of soft subgrades. This list of select materials is composed of:

1. Breaker run stone
2. Breaker run stone with geogrid
3. Grade 1 granular backfill
4. Grade 2 granular backfill
5. Pit run sand and gravel
6. Pit run sand and gravel with geogrid
7. Flyash, lime and cement stabilization
8. Salvage materials or industrial by-products with optional geogrid

In developing the testing philosophy, an approach that would yield general relationships that can be adapted to specific materials based on laboratory material property characterization was adopted rather than testing these 8 alternative materials. Furthermore, use of field data to validate the approach is critical. Thus, the available field test sections and materials constrained the choices. Therefore,, a generalized approach was developed using the large-scale laboratory experiments with the results validated in the field. This approach can be applied to other granular materials, chemical stabilization methods, or geosynthetics using the procedures described in this report. Thus, although tests were not conducted on each of the

materials listed above, the method we developed can be used to design with any of the materials.

Five materials were used in the experimental program: crushed rock (referred to as “breaker run”, Grade 2 granular backfill (referred to as “Grade 2”), bottom ash, foundry slag, and foundry sand. The breaker run rock and Grade 2, which are derived from dolostone (Mudrey et al. 1982), were retrieved during re-construction of a portion of Wisconsin State Highway (STH) 60 where field tests to evaluate working platform materials were conducted. The industrial byproducts were obtained from local industries.

Breaker run is defined by the Wisconsin Department of Transportation (WisDOT) as large-sized aggregate resulting from crushing of rock, boulders, large stone, or salvaged concrete that is not screened or processed after initial crushing (WisDOT 1996). Grade 2 is crushed or natural aggregate that is screened to meet the Gradation No. 2 requirements for granular backfill stated in WisDOT’s *Standard Specifications for Highway and Structure Construction* (WisDOT 1996). Bottom ash is a by-product of coal combustion in electrical power plants, whereas foundry slag and foundry sand are by-products of the gray iron casting industry. Bottom ash and foundry slag are well-graded coarse-grained sand-like materials. The foundry slag used in this study is referred to as tap slag, and is produced as a result of cupola water quenching. Foundry sand is a mixture of uniformly graded sand, a small fraction of binding agent, and combustible additives (Abichou et al. 2000). The foundry sand used in this study included 10% bentonite as the binder and < 4% “seacoal” (powdered coal) as the combustible additive.

Particle size characteristics and other physical properties of the materials are summarized in Table 1.1, along with “soil” classifications from the Unified Soil Classification System (USCS) and the American Association of State Highway and Transportation Officials (AASHTO) system. The particle size distribution curves are shown in Fig. 1.1 along with WisDOT’s Grade 2 gradation requirements (Fig. 1.1a). All of the materials are coarse-grained and classify as gravel (breaker run) or sand (bottom ash, foundry slag, and foundry sand) in the USCS. Grade 2 also classifies as sand in the USCS. However, the gravel nomenclature is retained herein because of its common usage. The materials range widely in particle size, with  $D_{60}$  between 29 mm (breaker run) and 0.23 mm (foundry sand).

Compaction curves for standard Proctor energy are shown in Fig. 1.2 for all materials except breaker run. Compaction tests could not be performed on the breaker run because of its large particle size. All of the materials except foundry sand are essentially insensitive to compaction water content. The fines and bentonite clay in foundry sand are responsible for its sensitivity to water content (Abichou et al. 2000). The California bearing ratio (CBR) of the materials ranges from 2 (foundry sand compacted 7% wet of optimum) to 80 (assumed for breaker run). Most of the CBRs range between 12 and 33.

The potential for leaching contaminants is an issue for bottom ash, foundry slag, and foundry sand. In Wisconsin, re-use of industrial by-products is controlled by Section NR 538 of the Wisconsin Administrative Code. This code requires leach testing of by-products and defines acceptable uses for such materials based on the leach test data. All of the by-products used in this study were tested by the suppliers

Table 1.1. Properties of working platform materials.

| Material     | Specific Gravity | D <sub>10</sub> (mm) | D <sub>60</sub> (mm) | C <sub>u</sub> | % Fines | USCS Symbol | AASHTO Symbol | Max. Dry Unit Weight (kN/m <sup>3</sup> ) |                           | Optimum Water Content per ASTM D 698 (%) | CBR                 |
|--------------|------------------|----------------------|----------------------|----------------|---------|-------------|---------------|---|---------------------------|--|---------------------|
|              |                  |                      |                      |                |         |             |               | Compaction per ASTM D 698                 | Vibratory per ASTM D 4253 |  |                     |
| Breaker Run  | NM <sup>a</sup>  | 0.25                 | 29                   | 116            | 3.1     | GW          | A-1-a         | NM <sup>a</sup>                           | NM <sup>a</sup>           | --                                       | 80 <sup>b</sup>     |
| Grade 2      | 2.65             | 0.090                | 6.0                  | 67             | 7.9     | SW          | A-1-a         | 22.6                                      | NM <sup>a</sup>           | --                                       | 33                  |
| Bottom Ash   | 2.65             | 0.060                | 1.9                  | 32             | 13.2    | SM          | A-1-b         | 15.1                                      | 13.7                      | --                                       | 21                  |
| Foundry Slag | 2.29             | 0.13                 | 2.0                  | 15             | 5.3     | SW-SM       | A-3           | 10.0                                      | 8.4                       | --                                       | 12                  |
| Foundry Sand | 2.55             | 0.0002               | 0.23                 | 1150           | 28.9    | SC          | A-2-7         | 16.1                                      | NM <sup>a</sup>           | 16                                       | 2 – 25 <sup>c</sup> |

Notes: <sup>a</sup>NM = not measured, <sup>b</sup>assumed CBR of breaker run, <sup>c</sup>un-soaked CBR of foundry sand varies with compaction water content.

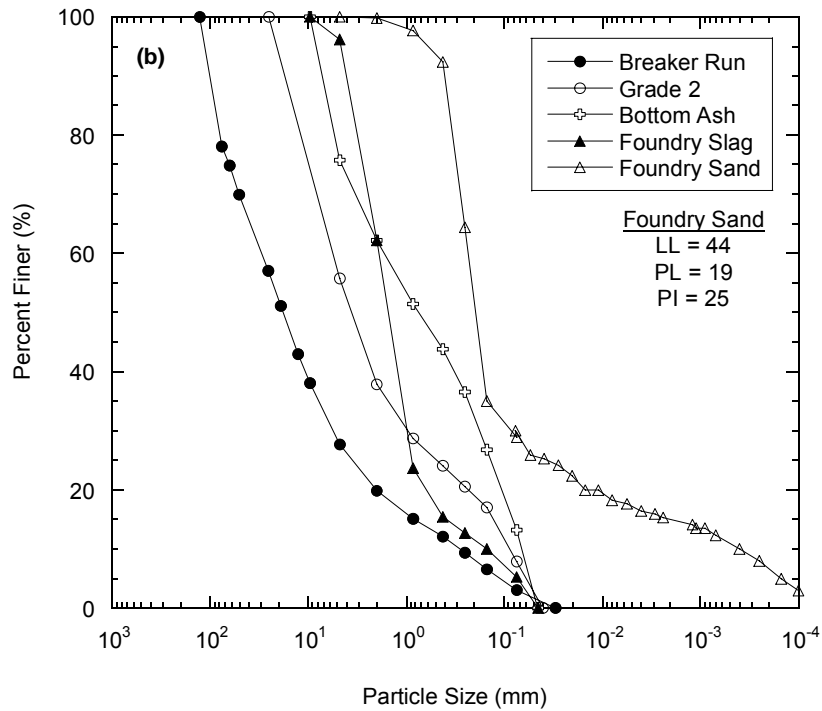
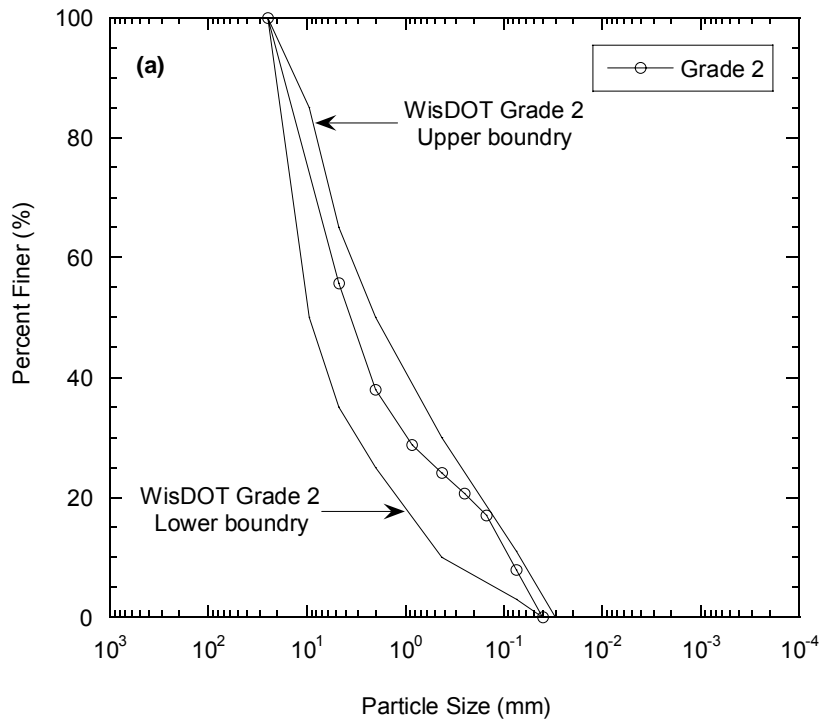


Fig. 1.1. Acceptable range of the particle size distribution for Grade 2 according to WisDOT (1996) along with particle size distribution of Grade 2 used in this study (a) and particle size distributions of working platform materials used in this study (b).

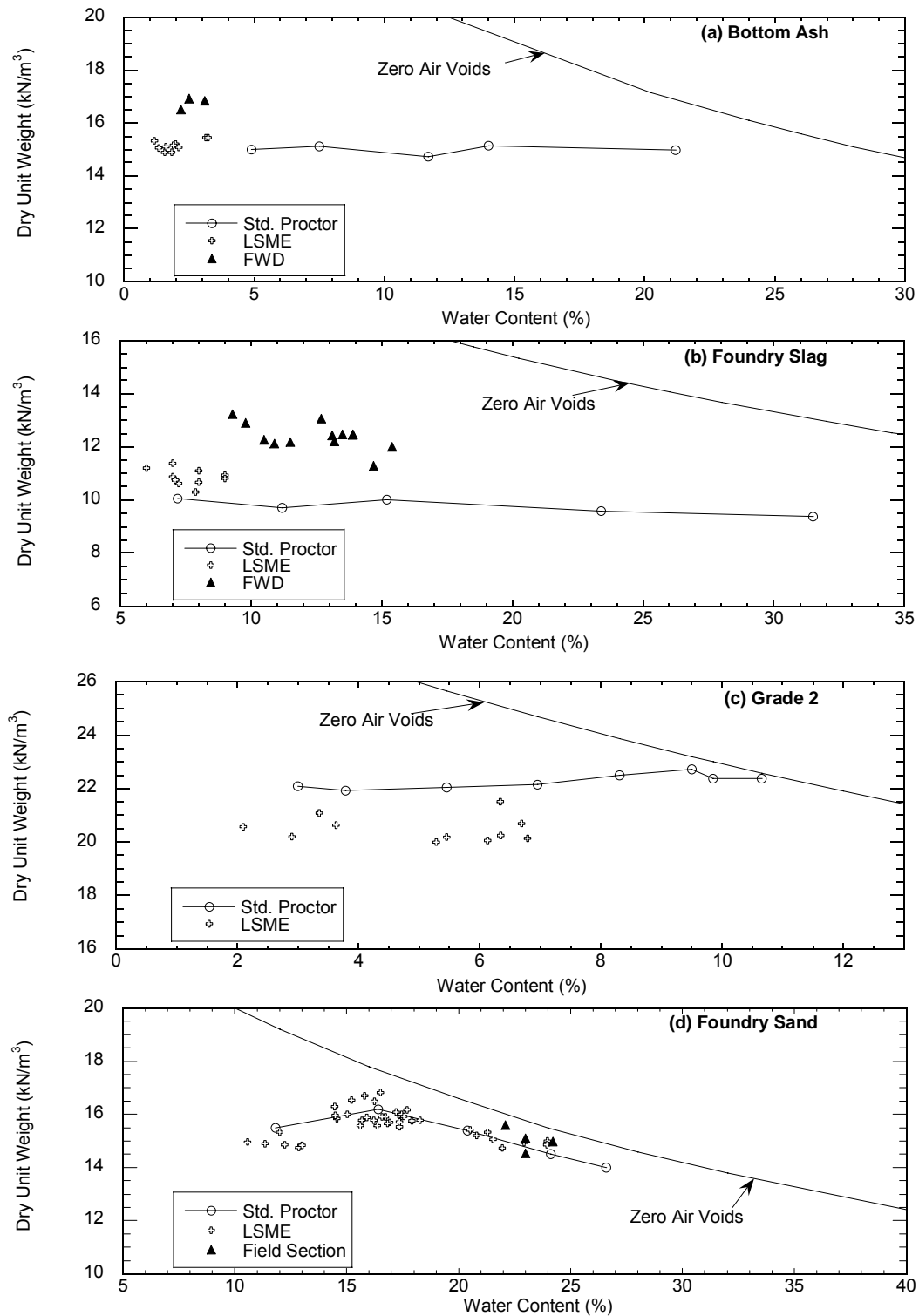


Fig. 1.2. Compaction curves and water content-dry unit weight data from field sections and LSME: bottom ash (a), foundry slag (b), Grade 2 (c) and foundry sand (d).

and found to be acceptable for use as “confined geotechnical fill” as defined in NR 538. This application includes pavement layers beneath an asphalt or concrete surface layer.

### **1.3 LARGE-SCALE TESTS**

Large-scale tests were conducted to evaluate how each of the working platform materials deflects under repetitive loads simulating construction traffic. These tests were conducted in the large-scale model experiment (LSME), a test apparatus for evaluating deflections during cyclic loading of a prototype-scale pavement structures (or part of a pavement structure) (Tanyu et al. 2003). A schematic of the LSME is shown in Fig. 1.3. The LSME consists of a pavement profile constructed in a 3 m x 3 m x 4 m test pit. A loading frame, actuator, and plate are used to simulate wheel loads. A detailed description of the apparatus can be found in Tanyu et al. (2003).

#### **1.3.1 Pavement Profile**

The pavement profile tested in this study consisted of three layers (from bottom to top): (i) dense uniform sand (2.5 m), (ii) simulated soft subgrade (0.45 m of expanded polystyrene foam), and (iii) the working platform material (0.22 to 0.90-m thick). Base course and asphalt were not included in the profile because the objective was to evaluate deflection of the working platform under construction loads prior to installation of base course.

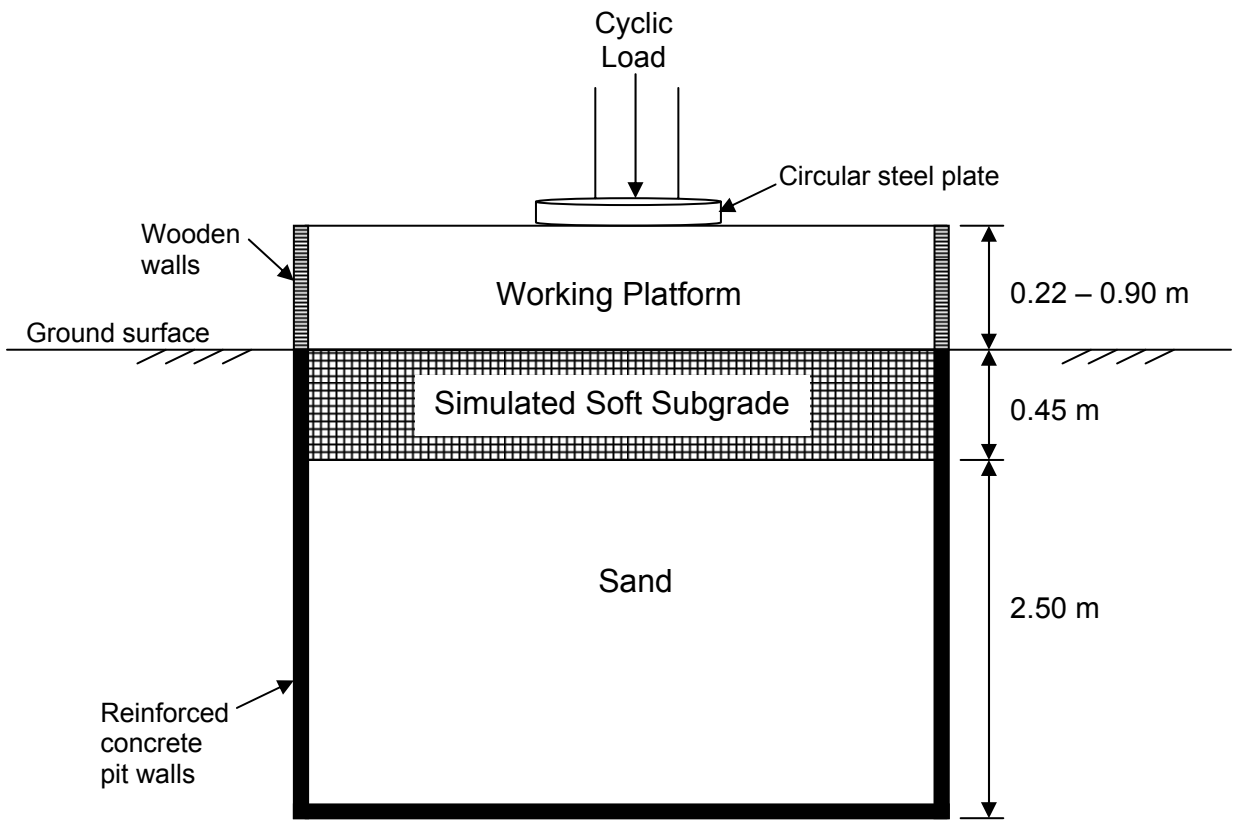


Fig. 1.3. Schematic cross section of Large-Scale Model Experiment (LSME).

The dense uniform sand layer at the base of the profile provides a firm foundation for the experiment, and simulates a deeper stiff layer. The expanded polystyrene (EPS) foam was used as poor subgrade in lieu of soft fine-grained soil to ensure uniformity, and to reduce the time and effort required to prepare experiments. Preliminary tests showed that the low-density EPS ( $17.1 \text{ kg/m}^3$ ) that was used has similar stress-strain behavior as typical soft subgrade soils found in Wisconsin (i.e., soils that have  $\text{CBR} \leq 1$ ) provided that the vertical stress on the EPS remains below 100 kPa (Tanyu et al. 2003). Negusse and Jahanandish (1993) also found that the stress-strain behavior of low-density EPS ( $21.0 \text{ kg/m}^3$ ) is comparable to that of soft inorganic clay of moderate plasticity.

To simplify construction, the EPS foam was placed in three layers of panels, each 0.15-m-thick, rather than as a single block. Data reported in Zou et al. (2000) suggest that deformation in the profile is unaffected by the use of panels instead of a single block of EPS. They show that block size and lateral restraint do not significantly affect the deformation behavior of EPS.

The working platform materials were placed in lifts 80 to 110 mm thick so that each material could be uniformly compacted with a vibratory plate compactor. For all materials except breaker run, each lift was compacted until the dry unit weight exceeded 95% of the maximum dry unit weight defined by the standard Proctor test (Fig. 1.2). Breaker run was compacted to the same dry unit weight ( $20.4 \text{ kNm}^3$ ) used at the field site (see subsequent discussion). Because of their insensitivity to water content during compaction, the breaker run, Grade 2, bottom ash, and foundry

slag were placed in the LSME at their existing water content. For foundry sand, LSME tests were conducted at three compaction water contents: optimum water content (i.e., 16%), 4% dry of optimum water content (12%), and the water content at which the foundry sand was placed at the field test site (23%, or 7% wet of optimum water content). The range of compaction water contents used for each material is shown in Fig. 1.2.

### **1.3.2 Loads and Deflections**

All of the pavement profiles were subjected to loads of high intensity and short duration simulating heavy truck traffic directly on the working platform during construction. The construction loads were selected to simulate the load applied by 4-axle dump trucks (70 kN per axle, and 35 kN per wheel set). These trucks normally have a tire pressure of approximately 700 kPa, which results in a contact area of 0.05 m<sup>2</sup> under a 35 kN load.

The 35-kN load was applied with a hydraulic actuator attached to a 25-mm-thick circular steel plate having a diameter of 250 mm (i.e., area = 0.05 m<sup>2</sup>) (Fig. 1.3). A haversine load pulse was applied that consisted a 0.1-s load period followed by a 0.9-s rest period. The same load pulse is used in the laboratory resilient modulus test (AASHTO 1994). One thousand load cycles were applied to simulate the typical level of construction traffic applied to a working platform (WisDOT 1996).

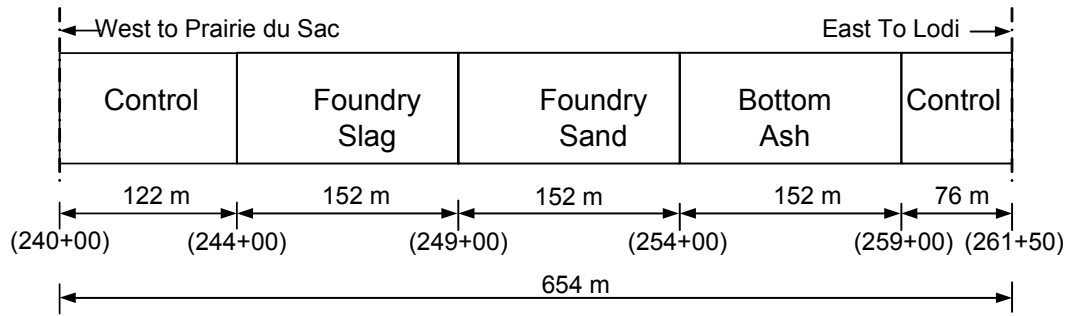
Vertical deflections of the pavement profile were measured directly underneath the loading plate and at distances of 300, 450, and 650 mm away from

the centerline of the actuator. Position transducers were used to measure the deflections during each loading cycle (Tanyu et al. 2003). Replicate measurements were made at distances of 300 and 450 mm on opposite sides of the loading plate. These replicate measurements generally differed by less than 10% at a given distance, and thus the average of these deflections was recorded. All of the load and deflection data were recorded by a CR9000 datalogger manufactured by Campbell Scientific Inc.

#### **1.4 FIELD METHODS**

Field tests were conducted on a 654-m long segment of Wisconsin State Highway (STH) 60 between Lodi and Prairie du Sac, Wisconsin that contains twelve test sections with different pavement profiles (2002). Five of these test sections were evaluated in this study. Plan and cross-sectional views of the test sections are shown in Fig. 1.4. Three were constructed using the industrial by-products (foundry slag, bottom ash, and foundry sand) as the working platform. Two are control sections (at the ends of the test site) where breaker run was used as the working platform.

The subgrade at the test site consists of lean silt (ML) or lean clay (CL). Laboratory tests show that all of the subgrade soils are soft (unconfined compressive strength between 100 and 150 kPa) and fairly uniform (Fig. 1.4) (Herr et al. 1995). An exception is the subgrade in the foundry sand section, which was notably softer than the subgrade in other sections.



| Foundry Slag   | Foundry Sand   | Bottom Ash  | Control  |
|--|--|---|--|
| 125 mm AC  | 125 mm AC  | 125 mm AC   | 125 mm AC  |
| 115 mm Grade 2 Base  | 115 mm Grade 2 Base  | 115 mm Grade 2 Base   | 115 mm Grade 2 Base  |
| 140 mm Salvaged Asphalt Base   | 140 mm Salvaged Asphalt Base   | 140 mm Salvaged Asphalt Base  | 140 mm Salvaged Asphalt Base   |
| 840 mm Foundry Slag Working Platform<br><br>$w = 12.5\%$<br>$\gamma_d = 12.4 \text{ kN/m}^3$ | 840 mm Foundry Sand Working Platform<br><br>$w = 23.2\%$<br>$\gamma_d = 15.0 \text{ kN/m}^3$ | 600 mm Bottom Ash Working Platform<br><br>$w = 2.6\%$<br>$\gamma_d = 17.1 \text{ kN/m}^3$ | 840 mm Breaker Run Working Platform<br><br>$w = 6.3\%$<br>$\gamma_d = 20.1 \text{ kN/m}^3$ |
| Subgrade   | Subgrade   | Subgrade  | Subgrade   |
| <u>ML-CL (A-4)</u><br>$w = 24.5\%$<br>LL = 30<br>PL = 22<br>$\gamma_d = 14.2 \text{ kN/m}^3$ | <u>ML-CL (A-4)</u><br>$w = 23.3\%$<br>LL = 34<br>PL = 24<br>$\gamma_d = 15.6 \text{ kN/m}^3$ | <u>CL (A-6)</u><br>$w = 24.9\%$<br>LL = 37<br>PL = 23<br>$\gamma_d = 14.4 \text{ kN/m}^3$ | <u>CL (A-6)</u><br>$w = 25.2\%$<br>LL = 46<br>PL = 26<br>$\gamma_d = 14.1 \text{ kN/m}^3$  |

(Not to scale)

Fig. 1.4. Pavement profiles and properties of subgrade and working platforms at STH 60 field site.

All of the working platform materials were placed in 150-mm-thick lifts and compacted with a tamping foot compactor until the dry unit weight exceeded 95% of that obtained with a standard Proctor test. The dry unit weight and the water content of each layer were measured periodically with a nuclear density gage. Water content and dry unit weights measured during construction are shown in Fig. 1.2.

Deflections in each working platform material were measured soon after the working platform materials were placed and before placement of any overlying layers. The deflections were measured using a rolling wheel deflectometer (RWD), which is a rolling platform for measuring deflections imposed by a single wheel load (Andren and Lenngren 2000). A test wheel (single G286 truck tire inflated to 760 kPa) mounted to a steel frame is loaded by water filled tanks (load = 53 kN). As the RWD passes over the working platform, total and plastic (non-recoverable) deflections of the working platform are measured using rotational potentiometers. Total deflections are recorded every 0.3 m along the alignment during a RWD test.

The RWD tests were conducted by Croveti and Schabelski (2001) using the RWD designed and fabricated at Marquette University. A detailed description of the RWD can be found in Croveti and Schabelski (1999).

## **1.5 RESULTS AND ANALYSIS**

### **1.5.1 Total Deflection Basins**

A typical graph showing total deflection ( $\delta_t$ ) under the loading plate of the LSME as a function of the number of load cycles is shown in Fig. 1.5 for working

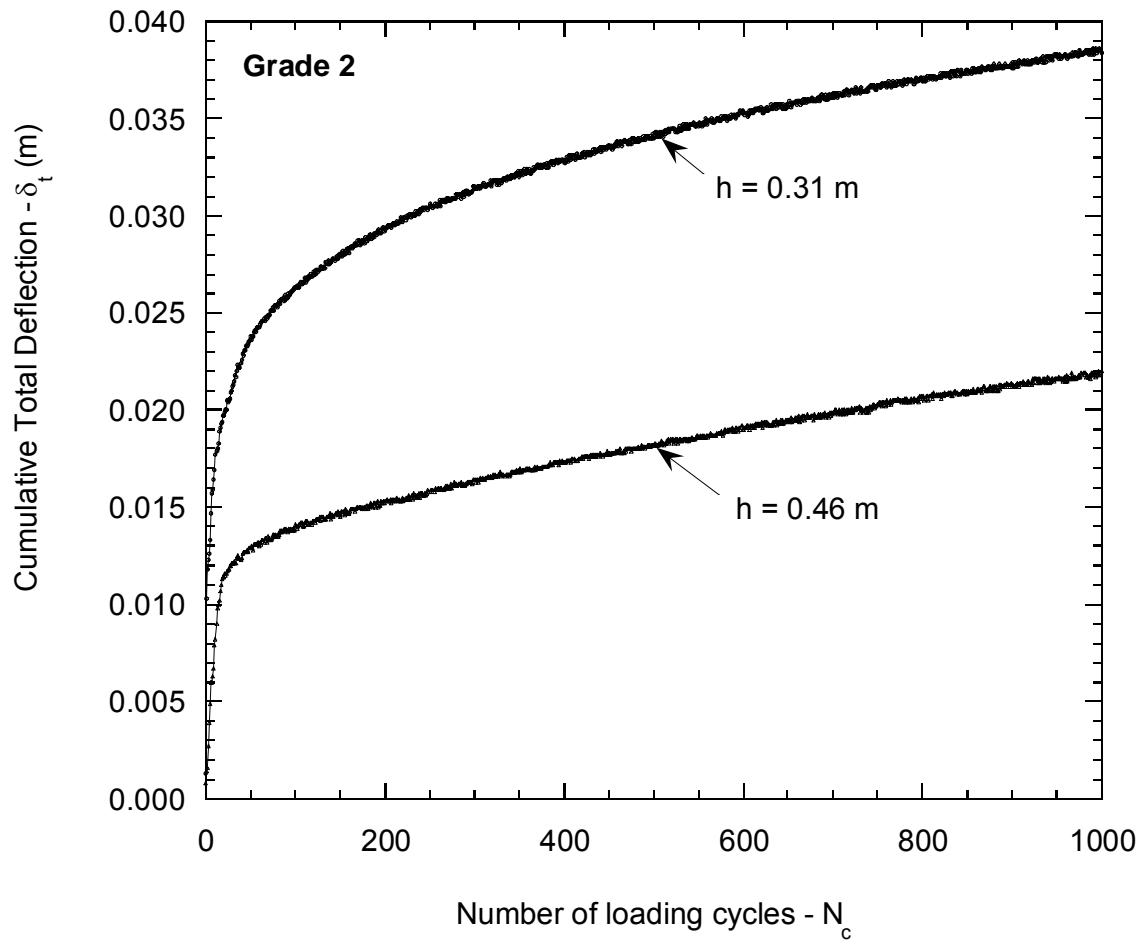


Fig. 1.5. Cumulative total deflection under the loading plate of the LSME as a function of number of load cycles for working platforms constructed with Grade 2 having a thickness ( $h$ ) of 0.31 and 0.46 m.

platforms constructed with Grade 2 that are 0.31-m and 0.46-m thick. Total deflection accumulates monotonically during both tests, with the greatest rate of accumulation within the first 40 cycles. In addition, the total deflection is smaller for the thicker layer for all loading cycles. Curves similar to those shown in Fig. 1.5 were obtained in all other tests. A summary of the maximum total deflection (measured during the 1000<sup>th</sup> load application) for each test is provided in Table 1.2. The deflections reported in Table 1.2 are sensitive to both the material being used and the thickness of the working platform.

The effect of layer thickness on the total deflection basin at 1000 cycles is shown in Fig 1.6a for working platforms constructed with bottom ash and breaker run. Breaker run and bottom ash are shown in Fig. 1.6a as illustrative examples; similar deflection basins were obtained for all materials that were tested. As the working platform becomes thicker, the total deflection decreases due to the additional stress distribution and corresponding reduction in strain in a thicker layer (Tanyu et al. 2003). The deflection basins in Fig. 1.6a also illustrate the relative stiffness of the working platform materials. For working platforms of equal layer thickness, deflections under the loading plate are smaller for breaker run than for bottom ash (i.e., the materials are not intrinsically equivalent because they have different stress-strain properties). However, a working platform can be constructed with bottom ash (or another alternative material) that is equivalent to a working platform of breaker run in terms of total deflection by using a thicker layer. For example, a 0.91-m-thick working platform of bottom ash yields the same total

deflection (33 mm under the loading plate) as a 0.31-m-thick working platform of breaker run.

The relative stiffness of the materials is illustrated in Fig. 1.6b, which shows deflection basins at 1000 cycles for each working platform material. The working

Table 1.2. Maximum total deflections directly underneath loading plate for all tests conducted in LSME along with parameters of Eq. 1.1.

| Material     |              | Thickness of working platform h (m) | Total deflection $\delta_t$ (mm) | Eq. 1 parameters |               |       |
|--------------|--------------|-------------------------------------|----------------------------------|------------------|---------------|-------|
|              |              |                                     |                                  | $\alpha$         | $\beta$       | $R^2$ |
| Breaker run  |              | 0.23                                | 46                               | 12.90            | -1.07         | 0.933 |
|              |              | 0.31                                | 32                               |                  |               |       |
|              |              | 0.46                                | 19                               |                  |               |       |
|              |              | 0.91                                | 14                               |                  |               |       |
| Grade 2      |              | 0.31                                | 38                               | 4.49             | -0.74         | 1.00  |
|              |              | 0.46                                | 22                               |                  |               |       |
| Bottom ash   |              | 0.46                                | 186                              | 3.44             | -0.39         | 0.943 |
|              |              | 0.69                                | 50                               |                  |               |       |
|              |              | 0.80                                | 48                               |                  |               |       |
|              |              | 0.91                                | 33                               |                  |               |       |
| Foundry Slag |              | 0.46                                | 187                              | 39.70            | -0.85         | 1.00  |
|              |              | 0.91                                | 83                               |                  |               |       |
| Foundry Sand | $w^a = 12\%$ | 0.46                                | 87                               | $57.05^b$        | $-1.07^b$     | 0.967 |
|              | $w = 16\%$   | 0.46                                | 17                               | 9.93             | -1.07         | 0.967 |
|              |              | 0.69                                | 13                               |                  |               |       |
|              |              | 0.91                                | 9                                |                  |               |       |
|              | $w = 23\%$   | 0.91                                | 472                              | $691^{b,c}$      | $-1.07^{b,c}$ | 0.967 |

Notes: <sup>a</sup>w = water content, <sup>b</sup>curve fit parameters are estimated based on the curve fit of foundry sand (w = 16%) due to limited data, <sup>c</sup>total deflection at 1,000 loading cycles extrapolated from data recorded between 0 and 40 loading cycles.

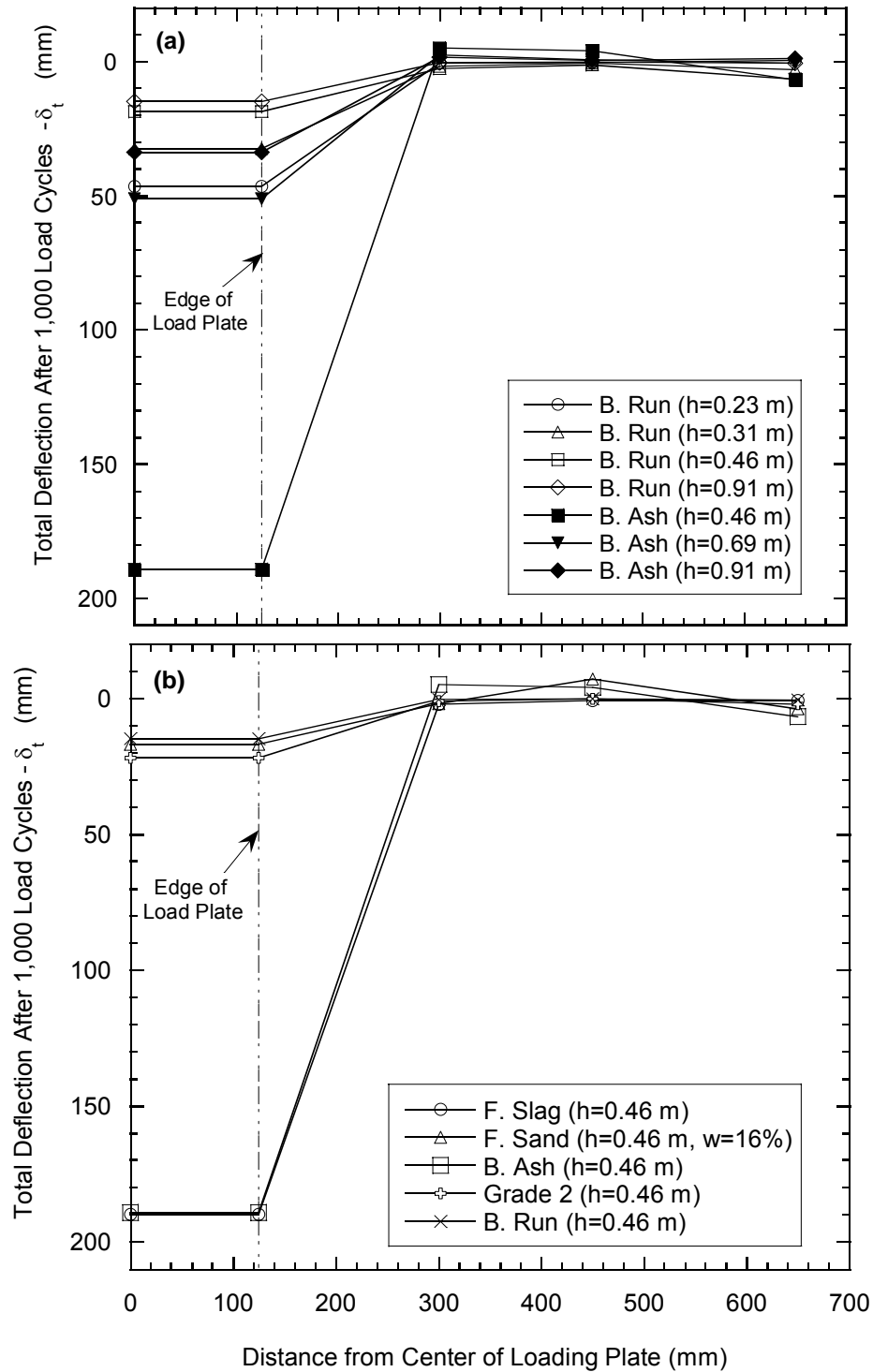


Fig. 1.6. Deflection basins for working platforms: (a) basins for breaker run and bottom ash showing the effect of thickness and (b) basins for all materials when the thickness of the working platform is 0.46 m(b).

platform is 0.46-m thick in each case. Deflections under the loading plate are almost ten times larger for bottom ash and foundry slag than those for breaker run and Grade 2. In contrast, the deflection basin for foundry sand prepared at optimum water content (i.e. 16%) is similar to those for breaker run and Grade 2.

The deflection basins also show the region of influence of the loading plate. The total deflection diminishes rapidly with distance, and is very small (< 10 mm) for all materials (Figs. 1.6 and 1.7) at a distance of 300 mm from the center of the loading plate (175 mm from the edge of the loading plate). Therefore, all subsequent comparisons are based on deflections directly under the loading plate.

Effect of compaction water content was only investigated for foundry sand, which is the only material studied that is sensitive to water content during compaction. LSME tests were conducted with foundry sand at three water contents: optimum water content (i.e., 16%), 4% dry of optimum water content (12%), and the water content at which the foundry sand was placed at the field test site (23%, 7% wet of optimum water content). Deflection basins at 1000 cycles for these water contents are shown in Fig. 1.7. The smallest total deflection under the wheel load was at optimum water content (i.e. 16%) and the largest total deflection was at 23% water content (7% wet of optimum water content). The total deflection for foundry sand compacted dry of optimum water content (12%) was also large compared to that for optimum water content (16%). For the test at 23% water content, the stroke limit of the actuator was reached within the first 40 loading cycles, requiring that the

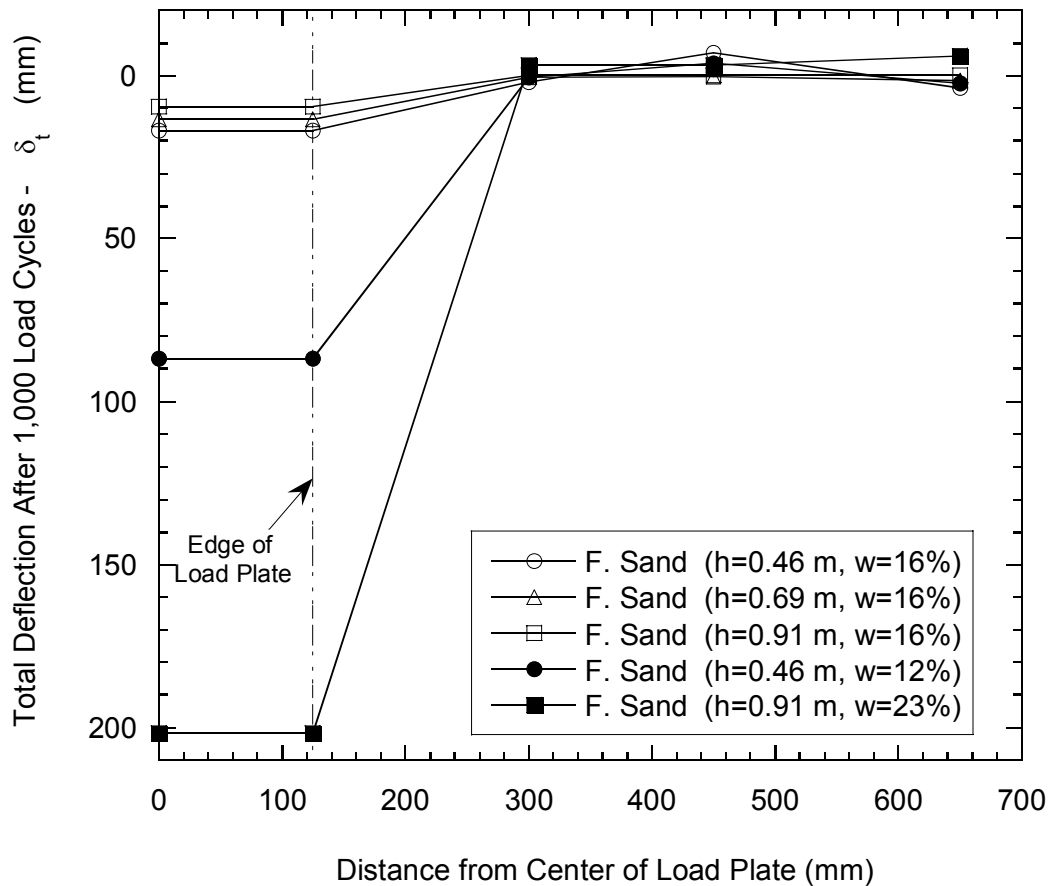


Fig. 1.7. Deflection basins for foundry sand prepared at optimum water content (16%), 4% dry of optimum water content (12%), and 7% wet of optimum water content (23%). The test at a water content of 23% was stopped at 40 loading cycles because the deflection was so large that the stroke limit of the actuator was reached.

test be terminated. If 1,000 cycles had been possible, a deeper deflection basin would have been obtained.

The sensitivity to water content observed for the foundry sand is consistent with observations reported by Kleven et al. (2000), who conducted CBR tests on a variety of gray-iron foundry sands compacted at water contents dry, wet, and at optimum water content. They show that the CBR is maximum at optimum water content, and lower at water contents wet or dry of optimum water content, for foundry sands having a 2  $\mu\text{m}$  clay content  $\geq 10\%$

### **1.5.2 Relationship Between Thickness and Maximum Total Deflection**

Defining equivalent working platforms required a functional relationship between the working platform thickness ( $h$ ) and total deflection ( $\delta_t$ ) at 1000 cycles obtained from the LSME for each material. These relationships were defined using the power function:

$$h = \alpha \delta_t^\beta \quad (1.1)$$

where  $\alpha$  and  $\beta$  are fitting parameters. A typical fit of Eq. 1.1 for bottom ash is shown in Fig. 1.8. A summary of  $\alpha$  and  $\beta$  for each material is in Table 1.2. The  $h$ - $\delta_t$  relationship can be used to identify the thickness of a working platform of alternative

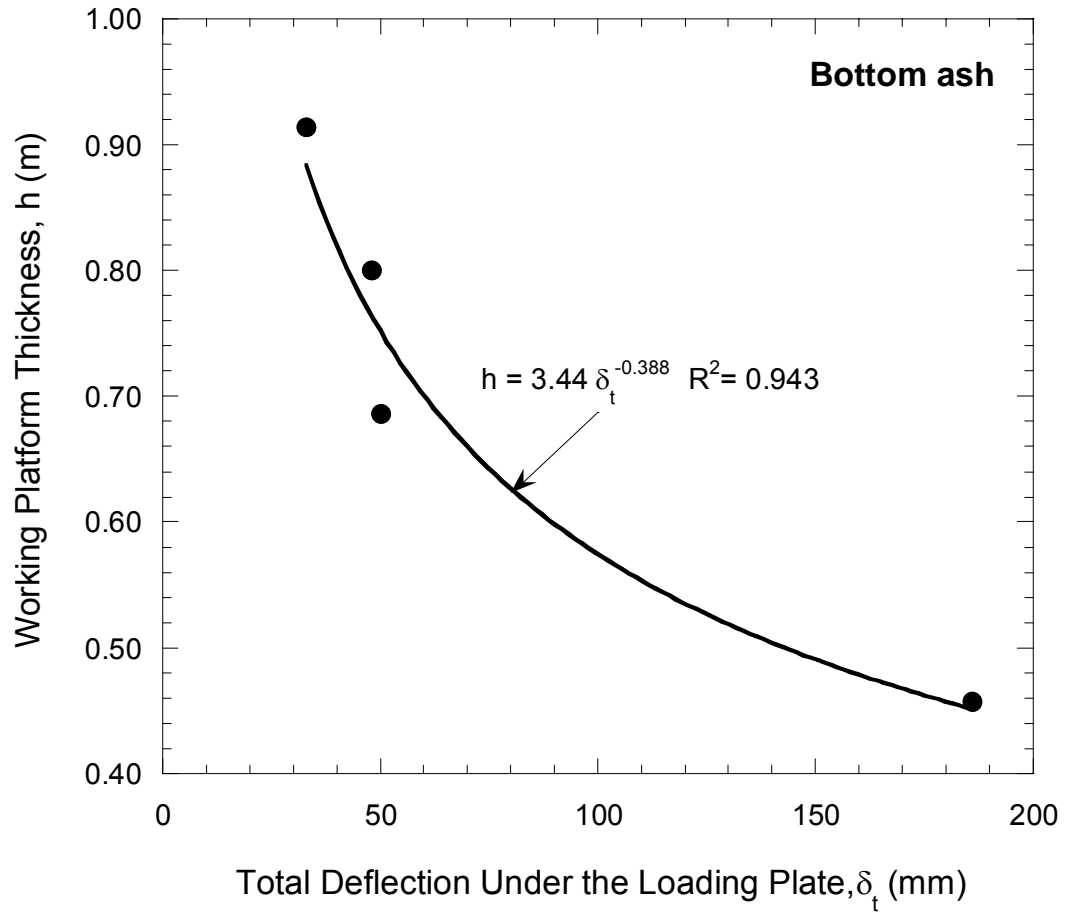


Fig. 1.8. Relationship between layer thickness and total deflection for working platforms constructed with bottom ash.

material that provides the same deflection as a working platform of breaker run.

Eq. 1.1 could not be fit to the data for foundry sand prepared at water contents of 12 and 23% because only one thickness was tested at each water content (0.46 m for 12%, 0.91 m for 23%). Thus, the rate of change of maximum total deflection (at 1000 cycles) with increasing thickness was assumed to be the same as that obtained from the tests with foundry sand at a water content of 16%, for which multiple thicknesses were tested. That is,  $\beta$  was assumed to be independent of water content, and  $\alpha$  was obtained directly from Eq. 1.1 using the measured total deflection and layer thickness. In addition, because the stroke limit was reached at 40 cycles when testing the foundry sand prepared at a water content of 23%, the deflection at 1000 cycles for this material was extrapolated from the deflection measured at 40 cycles. This extrapolating was made using a hyperbolic function relating total deflection ( $\delta_t$ ) and the number of loading cycles ( $N_c$ ):

$$\delta_t = \frac{N_c}{\mu + \lambda N_c} \quad (1.2)$$

where  $\mu$  and  $\lambda$  are fitted parameters. A hyperbolic function was used because its shape resembles the relationships between  $\delta_t$  and  $N_c$  that were measured (Fig. 1.5). Fits of Eq. 1.2 with  $R^2$  between 0.87 and 0.96 were obtained for all tests conducted with foundry sand. A check was also made to ensure that a fit of Eq. 1.2 using deflections from only 40 cycles could be used reliably to predict  $\delta_t$  at 1000 cycles.

This check was made by fitting Eq. 1.2 to the total deflections measured during the first 40 cycles ( $N_c=40$ ) for tests using foundry sand where 1000 load cycles were applied (i.e., all tests with foundry sand except those at a water content of 23%). Total deflections at  $N_c=1000$  were then predicted with Eq. 1.2, using the parameters fitted with  $N_c=40$ , and compared with the measured total deflection at  $N_c=1000$ . The predicted and measured total deflections at 1000 cycles differed by less than 3% (< 1.6 mm) for all tests, indicating that the extrapolation method is reliable.

### **1.5.3 Comparison of Total Deflections from RWD and LSME**

Deflections measured in the field with the RWD are shown in Fig. 1.9. Arithmetic means of the deflections measured with the RWD in each section are summarized in Table 1.3. The largest deflections were measured in the foundry sand section, and the smallest were measured in the breaker run sections. Deflections in the bottom ash and foundry slag sections were a factor of two to three higher than those in the breaker run sections. Deflections obtained from the LSME are also shown in Table 1.3. Because the working platforms had different thickness in the field and the LSME, deflections from the LSME reported in Table 1.3 are estimates obtained using Eq. 1.1, the parameters in Table 1.2, and the field thicknesses cited in Table 1.3.

A direct comparison cannot be made between deflections measured with the RWD and those measured in the LSME because different loads are used (53 kN vs. 35 kN), the number of loading cycles is different (i.e., 1 vs. 1000), and the working

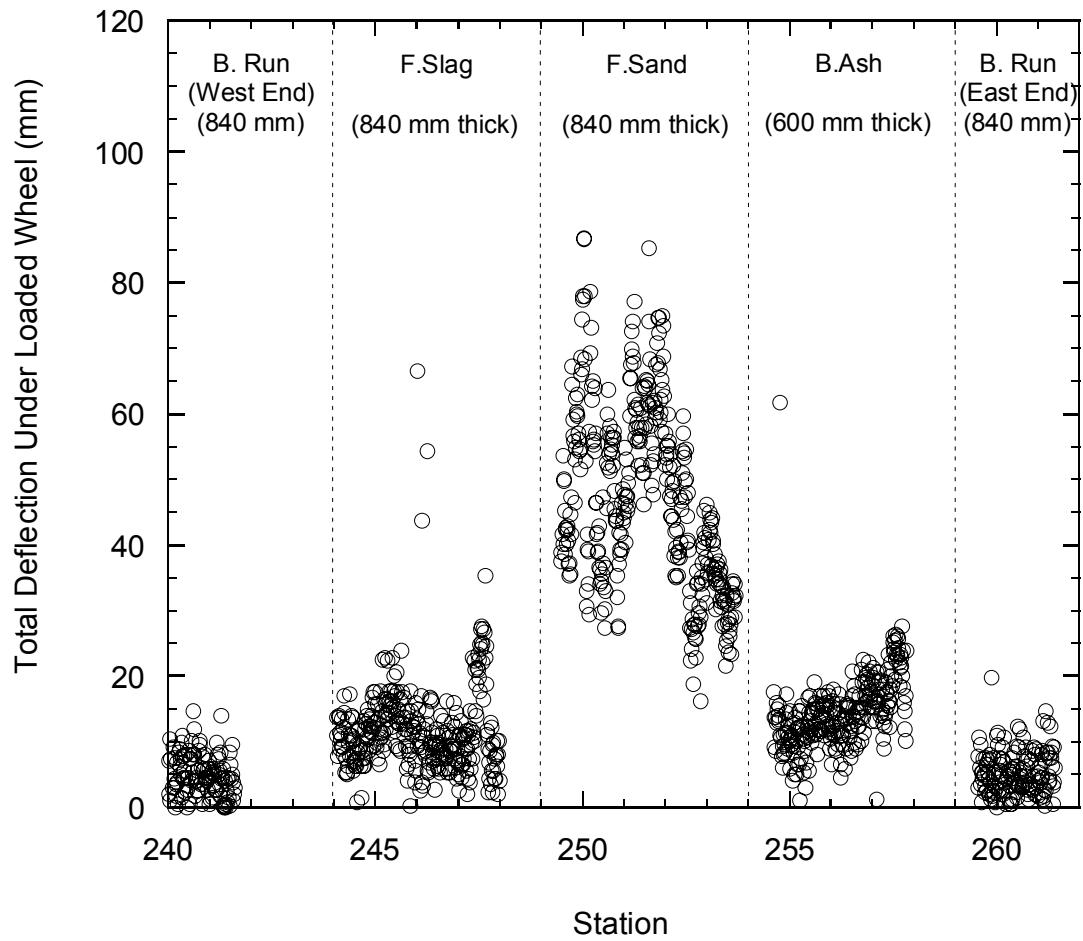


Fig. 1.9 Total deflections at the field site measured using the RWD.

Table 1.3. Total deflections obtained from RWD and estimated with Eq. 1.1 using parameters fitted to data from the LSME tests. Number of RWD measurements noted in parentheses.

| Materials              | Thickness at Field Site (m) | Total Deflection (mm)                                  |   |
|------------------------|-----------------------------|--|---|
|                        |                             | RWD <sup>a</sup><br>[ <sup>b</sup> N <sub>c</sub> = 1] | LSME<br>[ <sup>b</sup> N <sub>c</sub> = 1000] |
| Breaker run (West End) | 0.84                        | 4.0 ± 4.3 <sup>c</sup><br>(135 measurements)           | 12.8  |
| Breaker run (East End) |                             | 5.1 ± 3.6<br>(157 measurements)                        |   |
| Bottom Ash             | 0.60                        | 14.3 ± 5.8<br>(271 measurements)                       | 88.0  |
| Foundry Slag           | 0.84                        | 11.0 ± 8.2<br>(333 measurements)                       | 91.6  |
| Foundry Sand           | 0.84                        | 47.1 ± 14.3<br>(356 measurements)                      | 530.3   |

Notes: <sup>a</sup>Average total deflection from RWD tests, <sup>b</sup>N<sub>c</sub> = number of loading cycles, <sup>c</sup>± one standard deviation.

platforms in the field had different thickness than those in the LSME. Also, the dry unit weights in the field were slightly higher than those in the LSME (Fig. 1.2). However, a relative comparison of the deflections can be made by comparing the hierarchy of the deflections. The total deflections obtained from the RWD ( $\delta_{t,R}$ ) and LSME ( $\delta_{t,L}$ ) fall in the same order (Table 1.3), with the largest total deflections associated with foundry sand (water content =23%) and the smallest with breaker run. More importantly, the total deflections for the foundry slag and bottom ash are similar for both the RWD ( $\pm 3.3$  mm) and LSME ( $\pm 3.6$  mm) on average, even though the deflections for the LSME were estimated using Eq. 1.1. This favorable comparison suggests that equivalent working platforms can be selected using Eq. 1.1 fitted with deflection data from the LSME. That is, even though the materials are not intrinsically equivalent, a comparable working platform can be obtained with an alternative material provided the layer of alternative material has adequate thickness, as identified with Eq. 1.1.

#### **1.5.4 Comparison with Unpaved Road Design Methods**

A comparison was also made between the working platform thickness determined using Eq. 1.1 and the aggregate layer thickness obtained from the unpaved road design method described in Giroud and Noiray (1981). Working platforms and unpaved roads stabilized with an aggregate layer are similar in that both are intended to provide a sturdy platform for truck traffic when the subgrade is soft. The comparison was made with Giroud and Noiray's method because this

method includes the allowable deflection, load, number of loading cycles, and strength of the subgrade (i.e., variables considered in the LSME) as input, whereas most other guidelines (e.g., Steward et al. 1977, Bender and Barenberg 1978, Labuz 2000) apply only to a large number of truck passes (e.g., 10,000 or more) and/or heavier loads (80 kN axle loads). Thus, a direct comparison could be made with the method described by Giroud and Noiray, whereas direct comparisons are not possible with the other methods.

Giroud and Noiray's method (1981) defines the required aggregate layer thickness ( $h$ ) as a function of number of cycles ( $N_c$ ), applied load ( $P$  in N), rut depth ( $r$  in m), and undrained shear strength of the soft subgrade ( $c_u$  in Pa):

$$h = \frac{119.24 \log N_c + 470.98 \log P - 279.01r - 2283.34}{c_u^{0.63}} \quad (1.3)$$

When developing Eq. 1.3, Giroud and Noiray assumed that the aggregate would have CBR of 80 or larger. Thus, the comparison was made between the aggregate thickness computed using Eq. 1.3 and the thickness of a working platform of breaker run computed using Eq. 1.1. The total deflection was assumed to be 38 mm, which is a criteria being applied for working platforms in the Midwestern US. The subgrade was assumed to have CBR = 1 to represent the soft subgrade simulated in the LSME and the rut depth was assumed to equal the plastic deflection measured in the LSME, which was 70% of the total deflection on average (i.e.,  $r = 0.7 \times 38$  mm

= 0.026 m). The load  $P$  was set at 35,000 N,  $c_u$  was set at 31,000 Pa (based on recommendations in Giroud and Noiray for CBR =1), and  $N_c$  was set at 1000 cycles. For these inputs, Eq. 1.3 yields an aggregate thickness of 0.30 m, whereas Eq. 1.1 yields a working platform 0.27 m thick, a difference in thickness of only 30 mm.

## 1.6 EQUIVALENCY SELECTION METHOD

The relationships between thickness and total deflection defined by Eq. 1.1 and the parameters in Table 1.2 can be used to define equivalent thicknesses for alternative working platform materials. Equivalency, as defined here, requires that the total deflection of the alternative material ( $\delta_{ta}$ ) equal that of breaker run ( $\delta_{tb}$ ) under the same load at 1000 cycles. Equating total deflections (i.e.  $\delta_{ta} = \delta_{tb}$ ) using Eq. 1.1 yields:

$$h_a = \exp \left[ \frac{\beta_a}{\beta_b} \ln \left( \frac{h_b}{\alpha_b} \right) + \ln \alpha_a \right] \quad (1.4)$$

where  $h_a$  is the equivalent thickness of the alternative material,  $h_b$  is the thickness of breaker run,  $\alpha_a$  and  $\beta_a$  are the parameters in Eq. 1.1 for the alternative material, and  $\alpha_b$  and  $\beta_b$  are the parameters in Eq. 1.1 for breaker run. Eq. 1.4 was used to develop a design chart (Fig. 10) for selecting the thickness of an alternative material that will provide a working platform equivalent to a layer of breaker run. Curves are

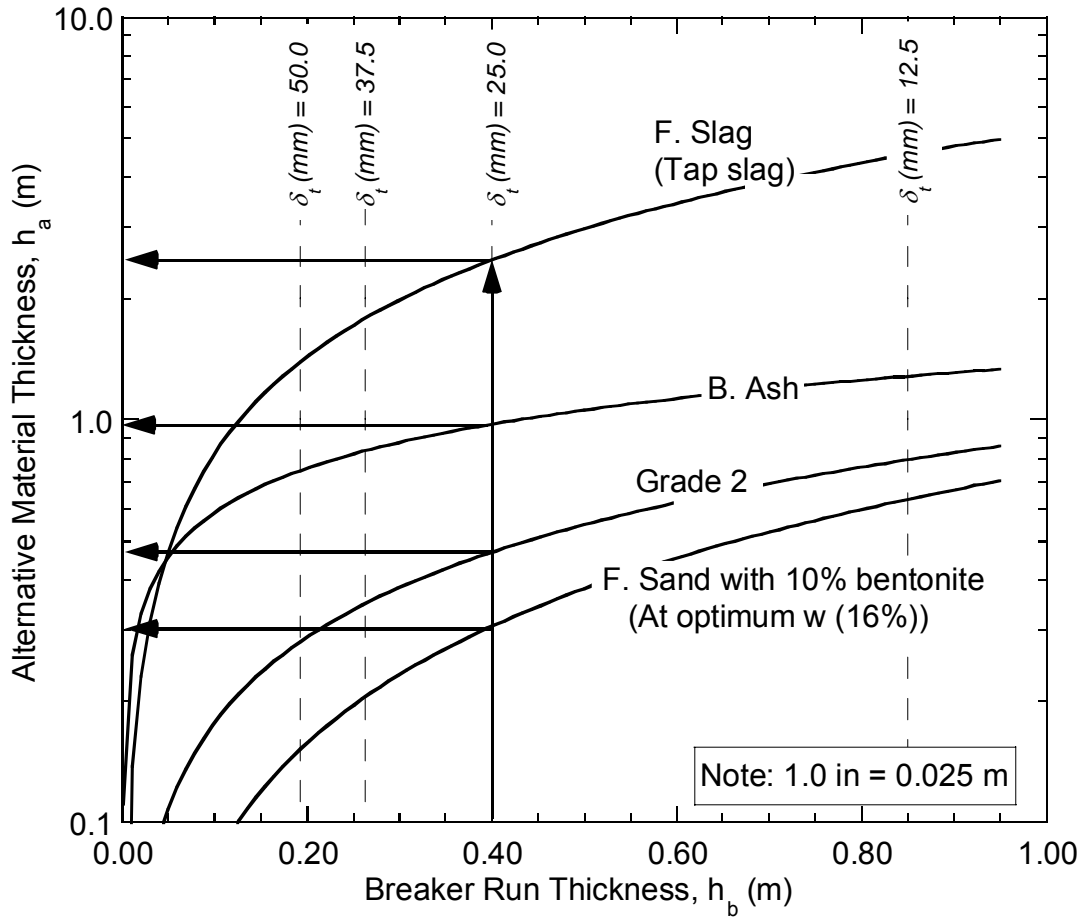


Fig. 1.10. Design chart relating thickness of each alternative material to thickness of breaker run.

shown for foundry sand (compacted at optimum water content), Grade 2, bottom ash, and foundry slag.

The following example explains how the design chart is used. Assume that the original design calls for a 0.4-m-thick working platform of breaker run, which will limit  $\delta_t$  to 25 mm. Thicknesses of each alternative material are then identified by extending a vertical line from the abscissa to each curve on the graph. For  $h_b = 0.4$  m, equivalent alternative working platforms can be constructed with 0.30 m of foundry sand (compacted at optimum water content), 0.45 m of Grade 2, 0.96 m of bottom ash, or 2.5 m of foundry slag (although more than 1.5 m is not economical). The thickness of a working platform constructed with foundry sand might be adjusted upward to 0.4 m (i.e., the same as breaker run) to account for variations in water content that may occur in the field.

The chart shown in Fig. 1.10 applies only to the alternative materials tested in this study. One approach to generalize the equivalency method is to relate the total deflections to readily measurable properties of working platform materials, such as CBR (i.e., a measure of total deflection under a large load analogous to a loaded working platform). Such a chart is shown in Fig. 1.11, which relates the ratio  $h_a/h_b$  to normalized CBR (unsoaked CBR of the alternative material  $\div$  CBR breaker run, which is assumed to be 80) for  $\delta_t = 12, 25,$  and  $50$  mm. The CBR assumed for breaker run has no practical consequence, because the CBR of breaker run only affects the scale of the abscissa in Fig. 1.11. The points in Fig. 1.11 correspond to  $h_a/h_b$  computed using Eq. 1.4. Smooth curves are drawn through the points for

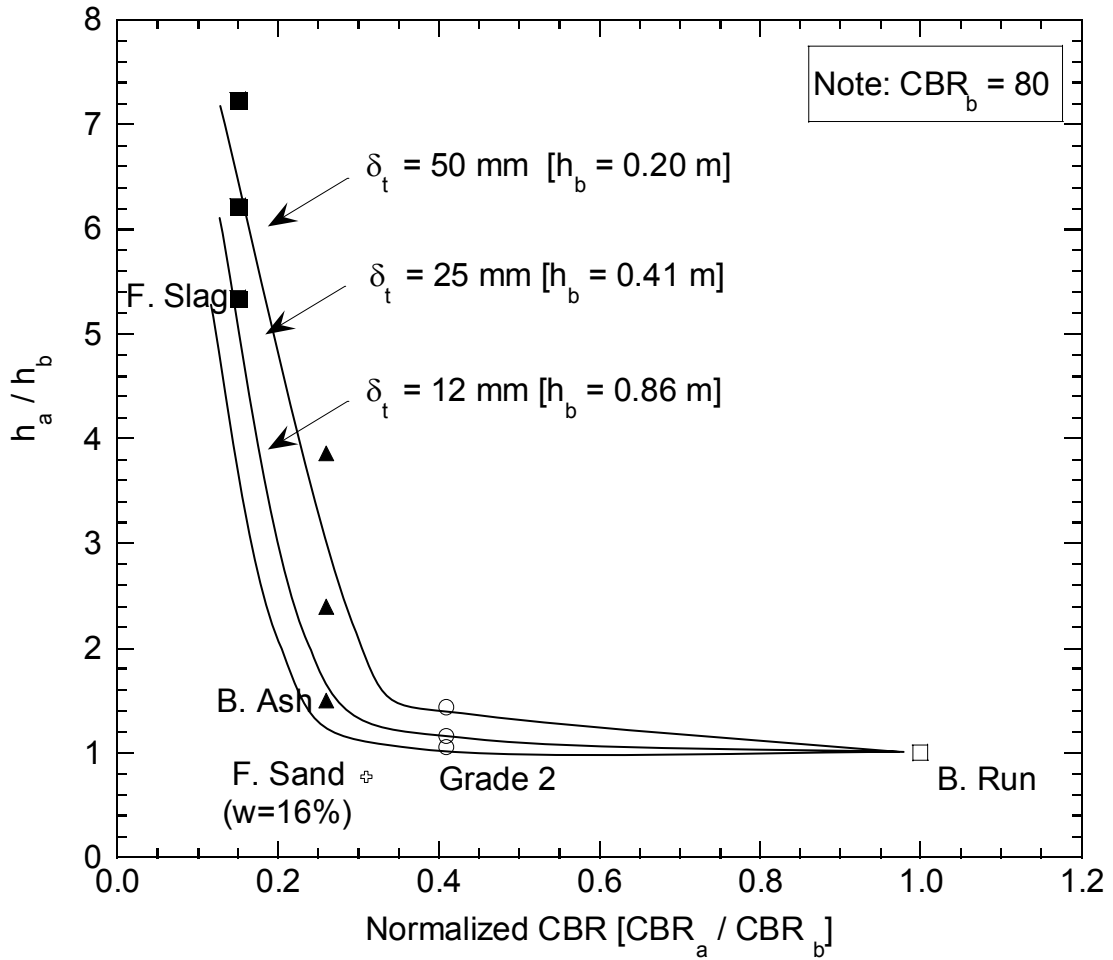


Fig. 1.11. Design chart relating ratio of thickness of working platform of an alternative material ( $h_a$ ) to the thickness of breaker run ( $h_b$ ) required to limit total deflections to 12, 25, and 50 mm as a function of normalized CBR (CBR of alternative material  $\div$  CBR of breaker run).

granular materials. The point corresponding to foundry sand was not included, because this point is inconsistent with the trends observed for the more granular materials.

Fig. 1.11 is conceptual. Additional tests have not yet been conducted to evaluate the generality of the curves and designers should keep in mind the conceptual nature of this graph when applying the equivalency approach. Nevertheless, the trends in Fig. 1.11 are reasonable. For each  $\delta_t$ , the required thickness decreases as the CBR of the alternative material increases. The graph also indicates that working platforms may need to be very thick for alternative materials having a CBR ratio  $< 0.25$ , particularly if a very small  $\delta_t$  is required. Thus, some materials may not be viable alternatives to breaker run in some projects because the required thickness will render the alternative material uneconomical. Site-specific criteria (e.g., type of highway, whether the working platform will be included in the pavement structural design as subbase, availability of materials, final elevations and required cut depth, etc.) should also be considered when designing working platforms with alternative materials.

## **1.7 CONSTRUCTION ISSUES**

The construction of alternative material sections in the field are described in another report (WHRP Project SPR #0092-45-98). In general, the handling, placement, and compaction of the bulk industrial byproducts did not present any special problems and were similar to natural aggregate with the exception of foundry

sand. The foundry sand used had a relatively high bentonite content (~10%) and showed sensitivity to moisture during construction. It was delivered somewhat wet and with the precipitation events at the site, it became difficult to compact and develop sufficient stiffness. However, with some drying it was possible to complete the construction of the foundry sand section. Kleven et al. (2000) investigated ferrous foundry sands in the Midwestern states from 14 different sources and found that the effective size ( $D_{10}$ ) ranged between 0.002 mm and 0.18 mm and the fines content ( $P_{200}$ ) ranges between 1.1% and 16.4%. The 2  $\mu\text{m}$  clay content varied from 0.8% to 10.0%. The active clay content of the clay-bonded excess system sands ranged between 5.1 and 10.2%. The specific foundry sand used in the test section is at the high end of the range reported for clay content of foundry sands. The field test sections were monitored at different intensity for 5 years. Further details of construction and performance of field sites based on the monitoring data collected can be found in WHRP Project SPR #0092-45-98 report.

## **1.8 SUMMARY AND CONCLUSIONS**

The objective of this study was to develop a method for selecting the thickness of four alternative materials used in lieu of “breaker run” (crushed rock) as a working platform for highway construction on very soft subgrade. Breaker run is commonly used for working platforms, and thus was selected as the reference material. Three industrial byproducts (bottom ash, foundry slag, and foundry sand) and Grade 2 granular backfill were used as alternative materials. A working platform

of alternative material was considered equivalent to that with breaker run if the total deflection of the alternative material was equal to the total deflection of breaker run under the same construction loading.

Large-scale model experiments were conducted on each of the working platform materials to define the relationship between total deflection and working platform thickness for a typical construction loading (1000 trips of a loaded 4-axle dump truck). A simulated very soft subgrade was used in the experiments so that the findings could be used conservatively for most soft subgrade applications. Results of the large-scale tests were used to develop design charts relating the thickness of an alternative material required to achieve the same total deflection as a working platform of breaker run. The method for selecting equivalent thicknesses was checked with field data from a rolling weight deflectometer (RWD) test and an unpaved road design method from the literature. Both comparisons were favorable.

One of the design charts relates thickness of the alternative material to CBR. This chart is conceptual because the curves have not yet been validated with additional data. Nevertheless, the trends are consistent in that a thinner working platform is required when the alternative material has higher CBR, and a thicker working platform is needed when the required deflection is smaller. The chart also shows that very thick working platforms may be required for alternative materials having a  $CBR < 20$ . Thus, some alternative materials may not be economical substitutes for working platforms constructed with crushed rock in some projects.

## 1.9 GUIDELINES FOR USING INDUSTRIAL BYPRODUCTS AS WORKING PLATFORM

The following steps are suggested in using select granular materials (e.g., Grade 1 granular backfill, Grade 2 granular backfill, pit run sand and gravel) and granular industrial byproducts (e.g., foundry sand, foundry slag, bottom ash) as equivalent substitute for breaker run working platform:

1. Identify economically feasible industrial byproduct. The design procedure given here is for granular
2. Determine its acceptability under Wisconsin Administrative Code NR538 for Beneficial Use of Industrial By-Products. This is accomplished by having a water leach test (*Standard Test Method for Shake Extraction of Solid Waste with Water* (ASTM D 3987) performed on the industrial by-product. This data can be provided by the waste generator. For an industrial byproduct to be acceptable in a confined application (e.g., covered with an asphalt pavement), aqueous concentrations of these species must not exceed “Category-4” standards stipulated in the *Wisconsin Administrative Code NR 538*. If the industrial by-product meets this environmental acceptability test, proceed to the material characterization.
3. Perform typical suite of material characterizations tests, i.e., grain size distribution, Standard Proctor compaction, and California Bearing Ratio (CBR) tests.

4. Using the compaction test results, specify field compaction like natural earthen materials.
5. Using the CBR performed on a compacted sample of the by-product at the specified field density, determine the normalized CBR relative to breaker run (i.e., divide by 80).
6. Using the normalized CBR, determine the thickness ratio from Fig. 1.11 for the design total settlement during construction. A total deflection of 25 to 50 mm are acceptable during construction for typical hauling truck loads.
7. To obtain the equivalent thickness of the by-product, multiply the thickness ratio with the estimated thickness of breaker run that would be typically required to keep the total deflections to the design value. It is assumed that this thickness is known on the basis of experience to the designer. If the resulting by-product thickness is excessive (i.e., more than 1.5 m), it may not be economical to use.
8. Construction is carried out like other granular materials. Closer moisture content control may be needed for foundry sand containing more than 6% bentonite.

## **2.0 REFERENCES**

AASHTO (1994), "Standard Method of Test for Resilient Modulus of Unbound Granular Base/Subbase Materials and Subgrade Soils," T 294, Protocol P46, American Association of State Highway and Transportation Officials, 794-807.

- Abichou, T., Benson, C., and Edil, T. (2000), "Foundry Green Sands as Hydraulic Barriers: Laboratory Study," *Journal of Geotechnical and Geoenvironmental Engineering*, ASCE, Vol. 126, No. 12, 1174-1183.
- Andren, A. and Lenngren, C. A. (2000), "Evaluating Subgrade Properties With a High-Speed Rolling Deflectometer," *Geotechnical Special Publication*, Pavement, Subgrade, Unbound Materials, and Nondestructive Testing, Vol. 98, 17-30.
- Bender, D. A. and Barenberg, E. J. (1978), "Design and Behavior of Soil-Fabric-Aggregate Systems," *Transportation Research Board*, 671, 64-75.
- Chou, Y. T. (1976), "Analysis of Subgrade Rutting in Flexible Airfield Pavements," *Transportation Research Record*, 616, 44-48.
- Claussen, A. I. M., Edwards, J. M., and Sommer, P. (1977), "Asphalt Pavement Design-The Shell Method," *Proceedings 4<sup>th</sup> International Conference on the Structural Design of Asphalt Pavements*, Vol. 1, 39-74.
- Crovetti, J. A. and Schabelski, J.P. (1999), Comprehensive Subgrade Deflection Acceptance Criteria, Phase I Draft Interim Report, WisDOT Highway Research Study #98-1.
- Crovetti, J. A. and Schabelski, J.P. (2001), Comprehensive Subgrade Deflection Acceptance Criteria, Phase III Final Report WI/SPR 02-01, WisDOT Highway Research Study #98-1, SPR # 0092-45-95.
- Edil, T., Benson, C., Bin-Shafique, M., Tanyu, B., Kim, W., and Senol, A. (2002), "Field Evaluation of Construction Alternatives for Roadway Over Soft Subgrade," *Transportation Research Record*, 1786, 36-48.
- Finn, F., Saraf, C. L, Kulkarni, R., Nair, K., Smith, W., Abdullah, A. (1986), "Development of Pavement Structural Subsystems," NCHRP Report 291, Transportation Research Board, National Research Council, Washington, DC.
- Giroud, J. P. and Noiray, L. (1981), "Geotextile-Reinforced Unpaved Road Design," *Journal of Geotechnical Engineering*, 107, 1233-1254.
- Herr, W. J., Hall, J. W., White, T. D., and Johnson, W. (1995), "Continuous Deflection Basin Measurement and Backcalculation Under a Rolling Wheel Load Using Scanning Laser Technology," *Proceedings ASCE Transportation Congress*, 600-611.
- Huang, Y. H. (1993), *Pavement Analysis and Design*, Prentice Hall, Englewood Cliffs, New Jersey.

- Kleven, J.R., Edil, T. B., and Benson, C. H. (2000), "Evaluation of Excess Foundry System Sands for Use as Subbase Material," *Transportation Research Record*, 1714, 40-48.
- Labuz, J. F. and Readon, J. B. (2000), "Geotextile-Reinforced Unpaved Roads: Model Tests," *Geotechnical Fabrics Report*, July Issue, 38-43.
- Li, D. and Selig, T. (1996), "Cumulative Plastic Deformation for Fine-Grained Subgrade Soils," *Journal of Geotechnical Engineering*, Vol. 122, No.12, 1006-1013.
- Monismith, C. L., Ogawa, N. and Freeme, C. R. (1975), "Permanent Deformation Characteristics of Subgrade Soils Due to Repeated Loading," *Transportation Research Record*, 537, 1-17.
- Monismith, C. L. (1976), "Rutting Prediction in Asphalt Concrete Pavements," *Transportation Research Record*, 616, Transportation Research Board, National Research Council, Washington, DC, 2-8.
- Mudrey, M. G., Brown, B. A., and Greenberg, J. K. (1982), *Bedrock Geologic Map of Wisconsin*, Geological and Natural History Survey, University of Wisconsin-Extension.
- Negussey, D. and Jahanandish, M. (1993), "Comparison of Some Engineering Properties of Expanded Polystyrene with Those of Soils," *Transportation Research Record*, 1418, 43-50.
- Shackel, B. (1973), "Repeated Loading of Soils—A Review," *Australian Road Research*, Vol. 5, No. 3, 22-49.
- Shook, J. F., Finn, F. N., Witczak, M. W., and Monismith, C. L. (1982), "Thickness Design of Asphalt Pavements-The Asphalt Institute Method," *Proceedings 5<sup>th</sup> International Conference on the Structural Design of Asphalt Pavements*, Vol. 1, 17-44.
- Steward, J. E., Williamson, R. and Mohny, J. (1977), *Guidelines for Use of Fabrics in Construction and Maintenance of Low-Volume Roads*, Forest Service, United States Dept. of Agriculture, Portland, OR.
- Tanyu, B. F., Kim, W. H., Edil, T. B., and Benson, C. H. (2003), "Comparison of Laboratory Resilient Modulus with Back-Calculated Elastic Moduli from Large-Scale Model Experiments and FWD Tests on Granular Materials," *Resilient Modulus Testing for Pavement Components, ASTM STP 1437, Paper ID 10911*, G. N. Durham, A. W. Marr, and W. L. De Groff, Eds., ASTM International, West Conshohocken, PA, 191-208.

- Thompson, M. R. and Nauman, D. (1993), "Rutting Rate Analyses of the ASSHTO Road Test Flexible Pavements," *Transportation Research Record*, 1384, 36-48.
- WisDOT (1997), Subgrade Design/Construction Process Review, District 1 Final Report, State of Wisconsin, Department of Transportation.
- WisDOT (1996), *Standard Specifications for Highway and Structure Construction*, State of Wisconsin, Department of Transportation.
- WisDOT (2003), *Facilities Development Manual*, State of Wisconsin, Department of Transportation.
- Wood, D. M. (1982), "Laboratory Investigations of the Behaviour of Soils under Cyclic Loading: A Review," *Soil Mechanics—Transient and Cyclic Loads*, John Wiley and Sons, New York, 513-582.
- Zou, Y., Small, J. C. and Leo, C. J. (2000), "Behavior of EPS Geofoam as Flexible Pavement Subgrade Material in Model Tests," *Geosynthetics International*, Vol. 7, 1-22.

## **CHAPTER TWO**

# **EQUIVALENCY OF GEOSYNTHETIC-REINFORCED AGGREGATE MATERIALS USED FOR WORKING PLATFORMS DURING PAVEMENT CONSTRUCTION**

### **2.1 INTRODUCTION**

The common pavement construction practice on soft fine-grained subgrades has been to undercut the soft subgrade and replace it with a layer of “select” granular materials to provide a working platform to support heavy equipments or truck loads during construction as well as in-service vehicular traffic loads. Excessive subgrade rutting during construction can impede placement of subbase, base and asphalt layers using heavy construction equipment. Previous studies on this issue have focused primarily on estimating the cumulative deflection of subgrade under long-term loading conditions (Monismith et al. 1975, Chou 1976, Finn et al. 1986, Thompson and Nauman 1993, Li and Selig 1996). Less attention has been placed on deformation of soft subgrade during construction, although soft subgrade soils have long been known to provide inadequate support for construction truck traffic. For example, in Wisconsin, construction on soft subgrade soils has been identified as a major issue affecting cost and scheduling due to problems associated with construction delays, change orders, additional costs, and contract administration problems (WisDOT 1997).

Consistent with the traditional practice, the most common “select” granular material is a broadly graded crushed rock with large particles referred to as “breaker run” (WisDOT 1996). The high cost of select materials such as breaker run has lead

to keen interest in alternative materials. Reinforcing the granular material with geosynthetics can permit reduction in the thickness of a granular working platform, resulting in potential cost savings (Montanelli et al. 1997, Zhao and Foxworthy 1999, Huntington and Ksaibati 2000). This benefit is particularly attractive in areas where granular pavement material sources are scarce or have long haul distances.

The objective of this study was to determine the degree of reinforcement provided by four alternative geosynthetics and the resulting reduction in thickness of working platforms constructed with granular materials that would result in the same cumulative total deflection as a layer of breaker run under typical construction loadings. The study was directed to respond to needs in Wisconsin, but the findings are applicable to other locations where breaker run is used. Alternative geosynthetic-reinforced working platforms that provide equal deflection as a working platform to that of breaker run are referred to herein as being “equivalent.” This definition of equivalency applies only to the cumulative total deflection during construction.

## **2.2 BACKGROUND**

The development of permanent strains in the working platform or subgrade under truck loads during construction can eventually result in excessive permanent surface deformation (i.e., rutting). Geosynthetics have been successfully used to provide a reinforced granular layer over soft subgrade, reducing plastic deformation or granular layer thickness for the same deformation and increasing the support of

heavy construction loads over a low strength subgrade during pavement construction stage (Giroud and Noiray 1981, Christopher and Holtz 1985, Miura et al. 1990, Fannin and Sigurdsson 1996). In the early years, design procedures for stabilizing or reinforcing unpaved roads were mainly incorporated with geotextiles and suggested that the geotextile with higher modulus could reduce the aggregate thickness where large rut depths (greater than 75 mm) were acceptable. The reported successful use of geosynthetics in unpaved road applications can be mainly traced to the following benefits: (1) cost savings by reducing the granular layer thickness compared to conventional methods, (2) ease of construction, and (3) improved short- and long- term structural performances of the road.

Geosynthetics can be used as subgrade or aggregate subbase reinforcements to aid in supporting heavy truck loads during construction by distributing a concentrated load over a larger area of the subgrade, thus avoiding local overloading of the bearing capacity (Holtz et al. 1995, Koerner 1998, Perkins 1999). Construction loads applied to the surface of the working platform during construction create a lateral spreading motion and thus tensile lateral strains in the aggregate layer. This lateral movement allows for vertical strains to develop leading to permanent surface deformation in the working platform. Geosynthetic reinforcements are designed primarily to address permanent surface deformations (i.e., rutting) and to reduce the working platform thickness, reducing or restraining lateral movement by shear interaction between geosynthetic and aggregate materials. Increase in lateral confinement and lower lateral strain result in an increase in the modulus of aggregate layer and improving vertical stress distribution

on the subgrade, corresponding reduction in vertical strain in the aggregate and on the top of the subgrade. Leng and Gabr (2002) demonstrated that approximately 20% to 30% of surface deformation was reduced and more distributed vertical stresses were transferred to the subgrade by using geogrid reinforcement, compared to that for the unreinforced aggregate layer.

Geosynthetics can stretch like a membrane as the subgrade deforms under construction load. This type of tensioned membrane mechanism is especially important when laying an aggregate layer on soft subgrade with a limited load bearing capacity. Significant rutting and the resulting spread of load by geosynthetics continue until the subgrade bears the distributed load without further non-recoverable deformation. The tensioned membrane effect may reduce the thickness of the working platform required for initial construction. However, this function is not appropriate for permanent paved roads where large rut depths cannot be tolerated and where bearing capacity failure is not permissible. Giroud et al. (1984) stated that even for unpaved roads where large displacement was acceptable (say, 0.075 m or 0.15 m), only a 10% reduction in pavement thickness from its unreinforced thickness could be made due to the membrane effect of the geogrid. In addition, friction (interlocking) between the aggregate base or subbase and geosynthetic surface, and between geosynthetic and subgrade surfaces helped to minimize lateral spreading of the aggregate material and subgrade. However, the actual contribution of each mechanism to the overall reinforcement provided to the pavement system has yet to be quantified.

## 2.3 MATERIALS

Two granular materials were used: a typical granular backfill referred to herein as “Grade 2” and a crushed rock referred to herein as “breaker run”. Grade 2 is commonly used as base course in Wisconsin and consists of a crushed rock screened to the gradation criteria shown in Fig. 2.1 (WisDOT 1996). Breaker run is defined by the Wisconsin Department of Transportation (WisDOT) as large-sized aggregate resulting from crushing of rock, boulders, or large stone that is not screened or processed after initial crushing. The breaker run rock and Grade 2 were retrieved during re-construction of a portion of Wisconsin State Highway (STH) 60. Both are derived from Cambrian dolostone in southern Wisconsin (Mudrey et al. 1982).

Particle size characteristics and other physical properties of the materials are summarized in Table 2.1. Their particle size distributions are shown in Fig. 2.1, along with WisDOT’s Grade 2 gradation requirements. All of the materials are coarse-grained and classified as well-graded gravel (breaker run) and sand (Grade 2) in the Unified Soil Classification System (USCS). According to the compaction curve for Grade 2 with standard Proctor effort conducted by Tanyu et al. (2003), Grade 2 is essentially insensitive to compaction water content. A compaction test could not be conducted on the breaker run because of its large particle size. Breaker run is assumed to show insensitivity to water content because of less fines (i.e., 3% to 5%) than Grade 2 (i.e., 8%). The fines in coarse-grained materials are responsible primarily for its sensitivity to water content.



Table 2.1. Properties of Grade 2 and Breaker Run in LSME Tests.

| Material    | Specific Gravity | Size Fractions <sup>a</sup> (%) |        |      |       | C <sub>u</sub> | USCS Symbol | Maximum Dry Unit Weight <sup>b</sup> (kN/m <sup>3</sup> ) | CBR             |
|-------------|------------------|---------------------------------|--------|------|-------|----------------|-------------|---|-----------------|
|             |                  | Cobble                          | Gravel | Sand | Fines |                |             |   |                 |
| Grade 2     | 2.65             | 0                               | 45     | 47   | 8     | 67             | SW          | 22.6  | 33              |
| Breaker Run | NM <sup>c</sup>  | 23                              | 49     | 25   | 3     | 116            | GW          | NM <sup>c</sup>   | 80 <sup>d</sup> |

<sup>a</sup> Soil fraction refers to the fraction of breaker run smaller than 75 mm (both breaker runs contained cobbles larger than 75 mm)

<sup>b</sup> Compaction per ASTM D 698.

<sup>c</sup> NM = not measured.

<sup>d</sup> Assumed CBR.

Four different geosynthetics (a geogrid, a woven geotextile, a non-woven geotextile, and a drainage geocomposite) were used in the study. Geogrid is chosen because geogrid is primarily a reinforcement geosynthetics. Woven geotextile provides reinforcement in a manner different than geogrid but also provides separation. Non-woven geotextile provides primarily separation and drainage but also expected to provide some reinforcement. Conventionally drain geocomposites are used primarily for drainage and they also provide separation and are expected to provide some reinforcement. As their reinforcement function is expected but not well known, the drainage geocomposite was also included to evaluate its reinforcement contribution. The geosynthetics, other than geogrid, used in this study provide also additional functions other than reinforcement that may be beneficial in extending the life of the pavement. However, only short-term reinforcement benefit during construction is considered in this investigation.

Mechanical properties of geosynthetics used in this study are summarized in Table 2.2. The wide width strength (ASTM D 4595) of each geosynthetic material in the machine and the cross-machine directions are compared in Fig. 2.2. The greatest tensile strength at the failure is obtained for the drainage geocomposite and the least strength is obtained for the geogrid with the least yield point elongation at the failure (i.e., 20% in the machine direction and 11% in the cross-machine direction). The largest elongations (i.e., 72% in the machine direction and 57% in the cross-machine direction) at the failure are observed for the non-woven geotextile. The geogrid was a high strength biaxial polypropylene geogrid (Tenax MS<sup>TM</sup> 724) with an aperture size of 32 mm to 45 mm in the machine direction and in

Table 2.2. Properties of Geosynthetics Used in LSME Tests

| Geosynthetic Type                                       |                  | Test                       | Property                   | Test Method     | Values <sup>g</sup> (XMD) |
|---|------------------|----------------------------|----------------------------|-----------------|---------------------------|
| TENAX 724 <sup>a</sup><br>Geogrid                       | MS <sup>TM</sup> | Wide Width<br>Tensile Test | Thickness                  | ASTM D 5199     | NM <sup>h</sup>           |
|   |                  |                            | Mass per Unit Area         | ASTM D 5261     | 253.1 g/m <sup>2</sup>    |
|   |                  |                            | Aperture Size <sup>e</sup> | NA <sup>f</sup> | 32 (45) mm                |
|   |                  |                            | Peak Tensile Strength      | GRI-GG1         | 17.2 (16.0) kN/m          |
|   |                  |                            | Yield Point Elongation     | GRI-GG1         | 20 (11) %                 |
|   |                  |                            | Offset Tangent Modulus     | ASTM D 4595     | 88.3 (115.0) kN/m         |
|   |                  | Pullout Test <sup>i</sup>  | Max. Pullout Force         |                 | 25 kN/m                   |
|   |                  |                            | Max. Front Displacement    | GRI-GG6         | 35.8 mm                   |
| AMOCO 2006 <sup>b</sup><br>Woven<br>Geotextile          | Style            | Wide Width<br>Tensile Test | Thickness                  | ASTM D 5199     | 0.7 mm                    |
|   |                  |                            | Mass per Unit Area         | ASTM D 5261     | 268.2 g/m <sup>2</sup>    |
|   |                  |                            | Wide Width Tensile         | ASTM D 4595     | 35.3 (42.3) kN/m          |
|   |                  |                            | Wide Width Elongation      | ASTM D 4595     | 26 (19) %                 |
|   |                  |                            | Offset Tangent Modulus     | ASTM D 4595     | 147.9 (292.2) kN/m        |
|   |                  | Pullout Test <sup>i</sup>  | Max. Pullout Force         |                 | 22 kN/m                   |
|   |                  |                            | Max. Front Displacement    | GRI-GT6         | 65.1 mm                   |
|   |                  |                            | Interaction Modulus        |                 | 338 kPa                   |
| AMOCO 4553 <sup>c</sup><br>Non-woven<br>Geotextile      | Style            | Wide Width<br>Tensile Test | Thickness                  | ASTM D 5199     | 2.7 mm                    |
|   |                  |                            | Mass per Unit Area         | ASTM D 5261     | 315.6 g/m <sup>2</sup>    |
|   |                  |                            | Wide Width Tensile         | ASTM D 4595     | 14.5 (21.8) kN/m          |
|   |                  |                            | Wide Width Elongation      | ASTM D 4595     | 72 (57) %                 |
|   |                  |                            | Offset Tangent Modulus     | ASTM D 4595     | 34.0 (36.8) kN/m          |
|   |                  | Pullout Test <sup>i</sup>  | Max. Pullout Force         |                 | 12 kN/m                   |
|   |                  |                            | Max. Front Displacement    | GRI-GT6         | 156.7 mm                  |
|   |                  |                            | Interaction Modulus        |                 | 77 kPa                    |
| TENAX Tendrain <sup>d</sup><br>Drainage<br>Geocomposite |                  | Wide Width<br>Tensile Test | Thickness                  | ASTM D 5199     | 12.7 mm                   |
|   |                  |                            | Mass per Unit Area         | ASTM D 5261     | 1700.6 g/m <sup>2</sup>   |
|   |                  |                            | Tensile Strength           | ASTM D 4595     | 50.9 (54.4) kN/m          |
|   |                  |                            | Tensile Elongation         | ASTM D 4595     | 57 (34) %                 |
|   |                  |                            | Offset Tangent Modulus     | ASTM D 4595     | 675.0 (200.0) kN/m        |
|   |                  | Pullout Test <sup>i</sup>  | Max. Pullout Force         |                 | 24 kN/m                   |
|   |                  |                            | Max. Front Displacement    | GRI-GT6         | 72.0 mm                   |
|   |                  |                            | Interaction Modulus        |                 | 333 kPa                   |

<sup>a</sup> Biaxial oriented polypropylene.

<sup>b</sup> Polypropylene slit-film.

<sup>c</sup> Polypropylene needle punched.

<sup>d</sup> Tri-planar polyethylene geonet with non-woven polypropylene geotextiles.

<sup>e</sup> As reported by the manufacturer.

<sup>f</sup> NA=no standard method available.

<sup>g</sup> Machine direction (XMD=cross-machine direction).

<sup>h</sup> NM = not measured.

<sup>i</sup> Cross-machine direction only.

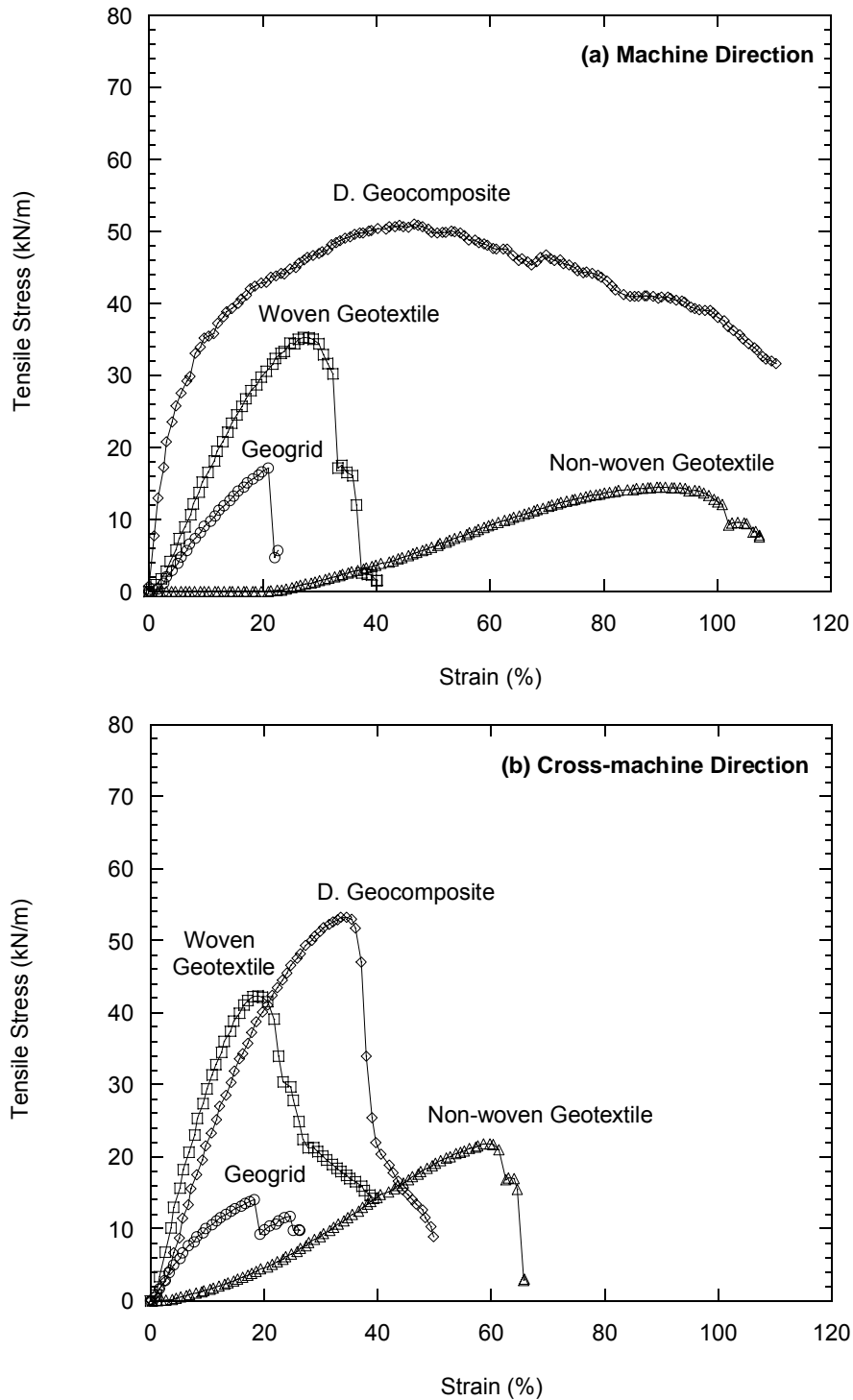


Fig. 2.2. Comparison of wide width strength (ASTM D 4595) for geosynthetics used in the LSME tests: (a) machine direction and (b) cross-machine direction.

the cross machine direction, respectively. The woven geotextile was a high strength polypropylene slit-film woven geotextile (Amoco 2006). The non-woven geotextile was also made of polypropylene and was needle punched (Amoco 4553). The geocomposite drainage material (Tenax Tendrain™) consists of a tri-planar polyethylene geonet with non-woven polypropylene geotextiles heat bonded to each side. The geonet consists of a triangular-shaped mesh structure with three sets of overlaid intersecting strands. The inner strands are thicker and heavier to provide higher resistance to compression and reinforcing capability.

## **2.4 PULLOUT TESTS**

Relative extensibility of the geosynthetics alone (not in soil) was characterized using wide-width tensile tests conducted in accordance with ASTM D 4595. Relative extensibility of the geosynthetics buried in soil (referred to as *in situ* extensibility herein) was characterized using pull-out tests conducted in accordance with Geosynthetic Research Institute (GRI) GG6 (geogrid) or GT6 (geotextiles and drainage composite). The pull-out box (1.52 m long, 0.61 m wide, and 0.41 m deep) described by Tatlisoz et al. (1998) and Goodhue et al. (2001) was used for the pull-out tests.

Displacements along the geosynthetic (0, 80, 220, and 420 mm from the front) were measured with linear variable differential transformers (LVDTs) attached to steel telltale wires encased in polyethylene tubing as described in Tatlisoz et al. (1998). For the pull-out tests, the geosynthetics (1.31 m x 0.41 m) were embedded

in Grade 2 (90 mm below, 300 mm above) compacted to 95% of maximum density per standard Proctor test. A normal stress of 6.3 kPa was applied (corresponding to a 0.30-m thick working platform of Grade 2 layer above the geosynthetic) and pull-out was conducted at 1 mm/min, with the pull-out load measured using a load cell mounted on the head.

An interaction modulus ( $M_i$ ) was computed for each of the geosynthetics using the pull-out data:

$$M_i = \frac{F_p/W L_g}{\Delta_f/L_g} \quad (2.1)$$

where  $F_p$  is the maximum pullout force,  $W$  is the width of the geosynthetic,  $L_g$  is the total length of the geosynthetic in the pullout test, and  $\Delta_f$  is the front displacement of the geosynthetic corresponding to  $F_p$ . The modulus  $M_i$  is an index of the *in situ* extensibility of the geosynthetics and the degree of engagement between a geosynthetic and granular material. Other descriptions of this interaction could have been used (e.g., the nonlinear interface shear stress-shear displacement relationship in Madhav et al. 1998 or Perkins and Cuelho 1999). However, a simple index of interface interaction based on directly measured quantities was preferred in this study.

## 2.5 LARGE-SCALE MODEL EXPERIMENT (LSME)

The large-scale model experiment (LSME) is a test apparatus for evaluating deflections during cyclic loading of a prototype-scale pavement structure (or parts of

it) in a manner that replicates field conditions as closely as practical. A schematic of the LSME is shown in Fig. 2.3. The LSME consists of a pavement profile constructed in a 3 m x 3 m x 3 m test pit. A loading frame, actuator, and plate are used to simulate wheel loads. A detailed description of the apparatus can be found in Tanyu et al. (2003).

### **2.5.1 Subgrade and Pavement Profile**

The subgrade and pavement profile tested in this study consisted of five layers (from bottom to top): (i) dense uniform sand (2.5 m), (ii) simulated soft subgrade (0.45 m of expanded polystyrene foam), (iii) 0.025 m of Grade 2, (iv) a geosynthetic layer, and (v) a layer of granular material simulating a working platform (0.30 m to 0.91 m). Base course and asphalt were not included in the profile because the objective was to evaluate deflection of the geosynthetic-reinforced working platform layer under traffic loads during construction.

The dense uniform sand layer at the base of the profile provides a firm foundation for the experiment and simulates a deeper stiff layer. The expanded polystyrene (EPS) foam was used to simulate a poor subgrade in lieu of soft fine-grained soil. EPS foam was selected to ensure uniformity and to reduce the time

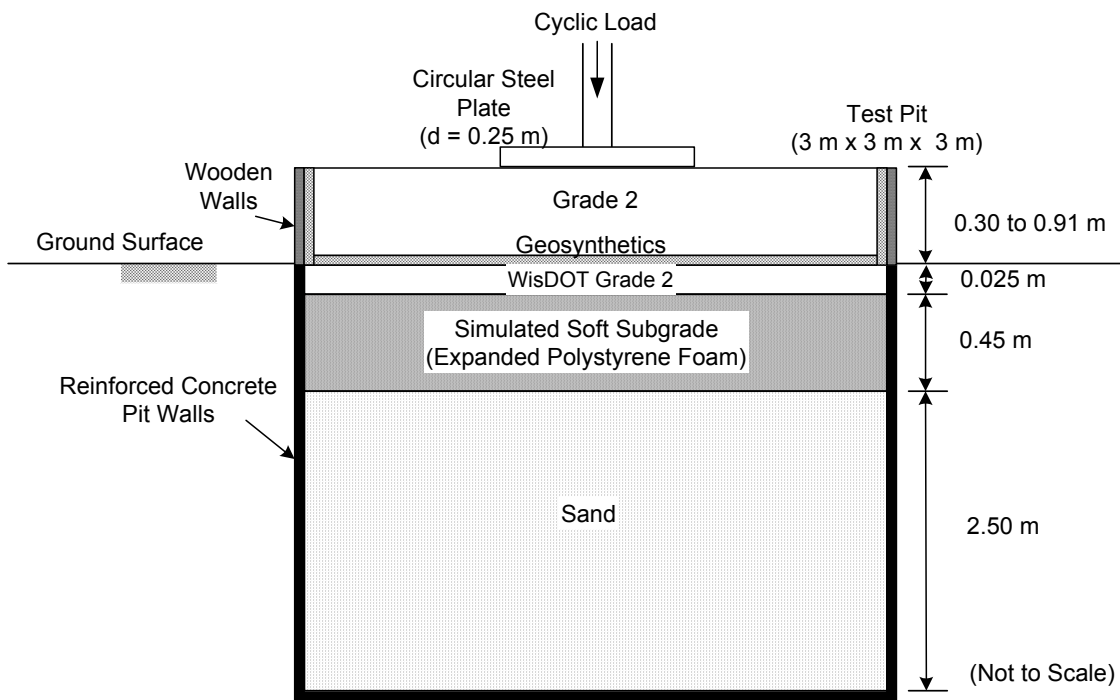


Fig. 2.3. Schematic cross section of large-scale model experiment (LSME).

and effort required to prepare experiments. Preliminary tests showed that the low-density EPS ( $17.1 \text{ kg/m}^3$ ) has similar stress-strain behavior as a typical soft subgrade soil found in Wisconsin (i.e., wet Antigo silt loam that has  $\text{CBR} \leq 1$ ) provided that the vertical stress on the EPS remains below 100 kPa (Tanyu et al. 2003). Negusse and Jahanandish (1993) also found the stress-strain behavior of low-density EPS ( $21.0 \text{ kg/m}^3$ ) comparable to that of a soft inorganic clay of moderate plasticity. The EPS foam was placed as three layers of panels, each 0.15-m-thick, to form a 0.45-m-thick layer. This approach was used instead of a single block of EPS to simplify construction. Zou et al. (2000) show that block size and lateral restraint do not significantly affect the deformation behavior of EPS. Thus, use of panels rather than a single block is not expected to affect deformation of the profile.

The materials placed on top of the EPS consisted of (i) 0.025-m thick layer of Grade 2 overlain by the geosynthetic reinforcing layer and 0.30- to 0.46-m thick Grade 2 working platform layer, or (ii) a 0.30-m to 0.91-m thick breaker run working platform layer without geosynthetic reinforcement.

The granular working platform materials were placed in lifts 0.08- to 0.11-m thick so that each material could be uniformly compacted with a vibratory plate compactor. For Grade 2, a nuclear gauge was used to measure the dry unit weight during compaction and each lift was compacted until the dry unit weight exceeded 95% of the maximum dry unit weight defined by the standard Proctor test (Tanyu et al. 2003). Breaker run was compacted to the same dry unit weight ( $20.0 \text{ kN/m}^3$ ) used at the field control site (see subsequent discussion). Because of their

insensitivity to water content during compaction, the Grade 2 and breaker run were placed in the LSME at their existing water content.

### **2.5.2 Loads and Deflections**

All of the pavement profiles in the LSME were subjected to loads of high intensity and short duration simulating heavy truck traffic directly on the working platform during construction. The construction loads were selected to simulate the load applied by 4-axle dump trucks (70 kN per axle, and 35 kN per wheel set). These trucks normally have a tire pressure of approximately 700 kPa, which results in a contact area of 0.05 m<sup>2</sup> under a 35 kN load.

The 35-kN load was applied with a hydraulic actuator attached to a 25-mm-thick circular steel plate having a diameter of 250 mm (i.e., area = 0.05 m<sup>2</sup>) (Fig. 3). A haversine load pulse was applied that consisted a 0.1-s load period followed by a 0.9-s rest period. The same load pulse is used in the laboratory resilient modulus test (AASHTO 1994). The dynamic motion of the actuator was provided by a 280-L/m MTS hydraulic actuator (MTS Model 244.22), having 100 kN of force rating and 168 mm of stroke. One thousand load cycles were applied to simulate the typical level of construction traffic applied to a working platform (WisDOT 2003).

Vertical deflections of the pavement profile were measured directly underneath the loading plate and at distances of 300, 450, and 650 mm away from the centerline of the actuator. Position transducers were used to measure the deflections during each loading cycles (Tanyu et al. 2003). Replicate measurements

were made at distances of 300 and 450 mm on opposite sides of the loading plate. These replicate measurements generally differed by less than 10% at a given distance, and thus the average of these deflections was recorded. All of the load and deflection data were recorded by a CR9000 datalogger manufactured by Campbell Scientific Inc.

### **2.5.3 Instrumentation**

The telltale movements in geosynthetics by the applied cyclic loads on Grade 2 surface were measured using calibrated linear variable differential transformers (LVDTs), which had a stroke of  $\pm 50$  mm and a nominal sensitivity of 1.5 V/V, with external signal conditioning. One end of a steel extension wire in the LVDT unit was attached to the geosynthetic at 0 mm, 130 mm, 255 mm, and 510 mm from the loading center in the cross machine direction.

Strain levels in the geosynthetic were measured with a series of resistance type strain gages attached on the upper and lower surfaces of the geosynthetic. The strain gage length of 6.35 mm and width of 3.18 mm (Micro-Measurement Division EP-08-250BG-120) were used for the geogrid and the drainage geocomposite, while 50.8 mm long and 4.78 mm wide strain gages (EP-08-20CBW-120) were used for the geotextiles. The gage had a 120-ohm resistance with a gage factor of 2.0 and could measure up to 1,000 microstrains under 2.5-V excitation voltage. Strain levels in cross-machine direction of the geosynthetic were measured

at five different locations from the center of the loading plate: 0 mm, 130 mm, 255 mm, 380 mm, and 510 mm.

For the non-woven and woven geotextiles where very steep strain gradients or stress concentration points are not expected, long strain gages were attached to the geosynthetic by using an adhesive (Armstrong A-12 Epoxy Resin part A and Part B) without altering locally the properties of the geosynthetic (Farrag 1999). Direct attachment of the strain gage using epoxy was inappropriate because of the potential stiffening effect of epoxy on long gages. Therefore, two ends of a thin plastic strip glued to the strain gage were attached to the geotextile via two aluminum end plates (Chew et al. 2000). A dog-bone shaped geomembrane specimen of equivalent cross-section and polymer type was used to mount strain gages to the geogrid and the drainage geocomposite because the geogrid rib or drainage geocomposite core was too narrow to mount a strain gage directly on it (Hayden et al. 1999). The dog-bone specimen was connected to the geogrid rib or the drainage geocomposite core (i.e., geonet) through clamps by two strips of 2-mm thick geomembrane bar that were bolted to adjacent ribs.

## **2.6 RESULTS AND ANALYSIS**

### **2.6.1 Pullout Tests**

The results of the pullout test on each geosynthetic with Grade 2 are shown in Fig. 2.4. At the normal stress used (i.e., 6.3 kPa), the pullout force for the geogrid, woven geotextile, and non-woven geotextile increases rapidly at low displa-

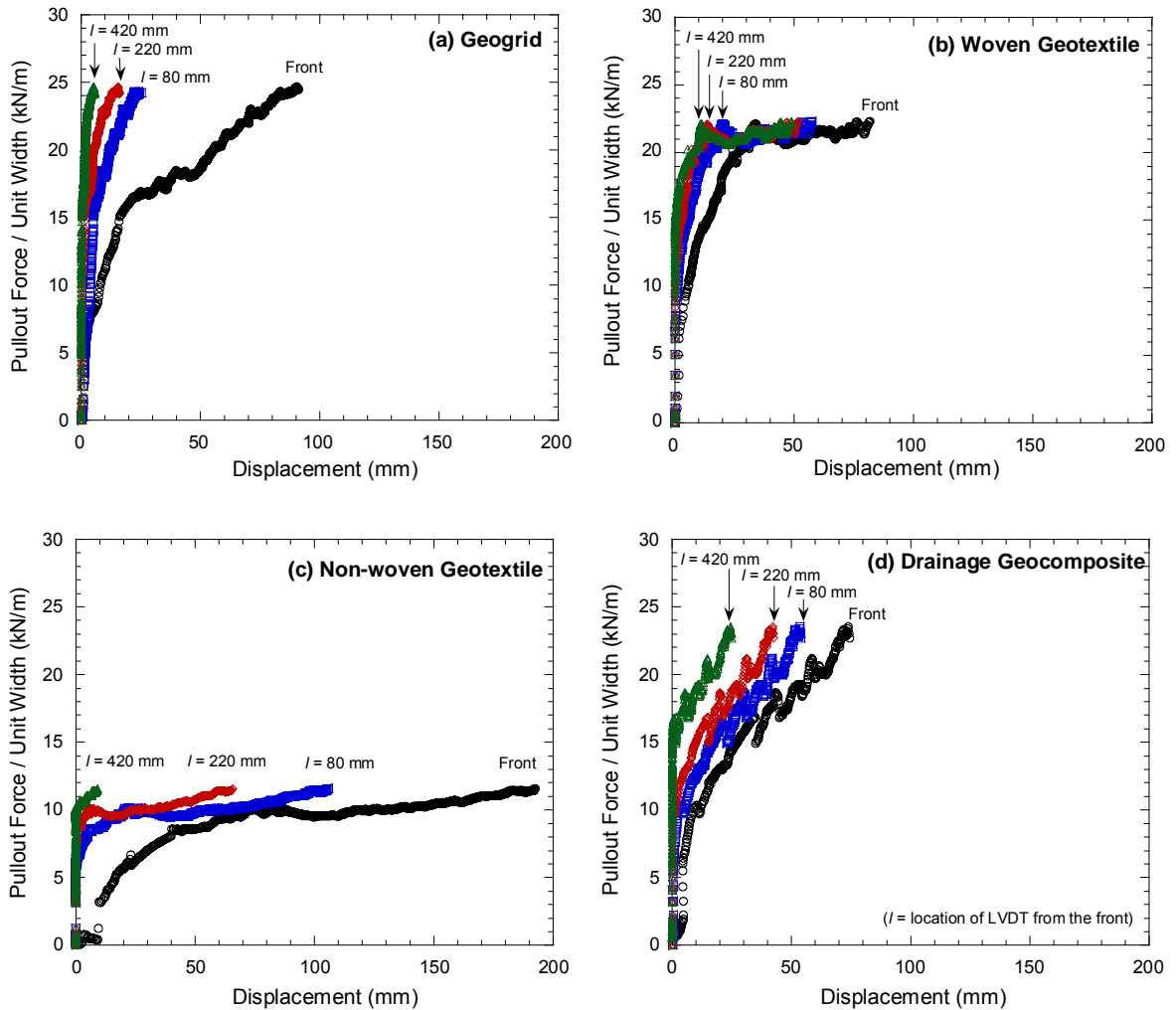


Fig. 2.4. Results of pullout test under 6.3 kPa of normal stress showing the relationship between force per unit width and displacement for: (a) geogrid; (b) woven geotextile; (c) non-woven geotextile; and (d) drainage geocomposite.

cements ( $< 20$  mm) and then become constant at higher displacements, without displaying a peak. On the other hand, it monotonically increases with nearly uniform relative displacement through the length of the drainage geocomposite with signs of progressive failure of the composite. In general, the pullout force at low normal stress becomes constants because the entire geosynthetic is displaced; thus, shear strength is mobilized almost completely along the entire length of the geosynthetic (Goodhue 2001). However, the drainage geocomposite with Grade 2 in this study shows a somewhat different displacement behavior than observed in other geosynthetics. All geosynthetics failed in tension in the pullout tests. The data obtained from the pullout tests are summarized in Table 2. The  $M_i$  ranges from 699 kPa (geogrid) to 77 kPa (nonwoven geotextile), indicating that the geogrid is the least extensible and the nonwoven geotextile the most extensible when embedded in Grade 2.

## **2.6.2 LSME Tests**

### **2.6.2.1 Total Deflection Basins**

Cumulative total deflections ( $\delta_t$ ) under the loading plate of the LSME as a function of the number of load cycles are shown in Fig. 5 for aggregate platforms having a thickness ( $h$ ) of 0.30 m or 0.46 m. Total deflection accumulates monotonically during the LSME tests for geosynthetic-reinforced platforms constructed with Grade 2 as well as for the unreinforced Grade 2 and the breaker run.

The deformation quickly increases at the onset of the loading cycle with the greatest rate of accumulation within the first 100 cycles. The deformation rate then decreases as the number of load cycles increases and a steady state condition is reached after approximately 200 load cycles. As shown in Fig. 2.5, geosynthetic reinforcements in aggregate platforms actually can limit the total deflection whereas unreinforced aggregate platforms (Grade 2 or breaker run) continue to accumulate total deflections with increasing loading cycles beyond 200 cycles. This effect is more evident in the thicker 0.46-m aggregate platforms. After 1,000 load cycles, the total deflections for the geosynthetic-reinforced platforms are reduced by 18% to 40% for the 0.30-m-thick and by 31% to 51% for the 0.46-m-thick platforms compared to the unreinforced Grade 2 platform. Furthermore, the total deflection is smaller for the thicker layer for all loading cycles.

#### **2.6.2.2 Effect of Layer Thickness on The Total Deflection Basins**

The effects of layer thickness and geosynthetic reinforcement on the total deflection basin at 1,000 load cycles are shown in Fig. 2.6a for Grade 2 platforms reinforced with two different types of reinforcement products: geogrid and non-woven geotextile. Geogrid and non-woven geotextile reinforced platforms are shown in Fig. 2.6a as illustrative examples; similar response was also obtained in the woven geotextile and the drainage geocomposite reinforced platforms that were tested. As the aggregate working platform becomes thicker, the total deflection decreases due to the additional stress distribution and corresponding reduction in strain in a thicker layer (Tanyu et al. 2003). The reduction rate in the total deflection

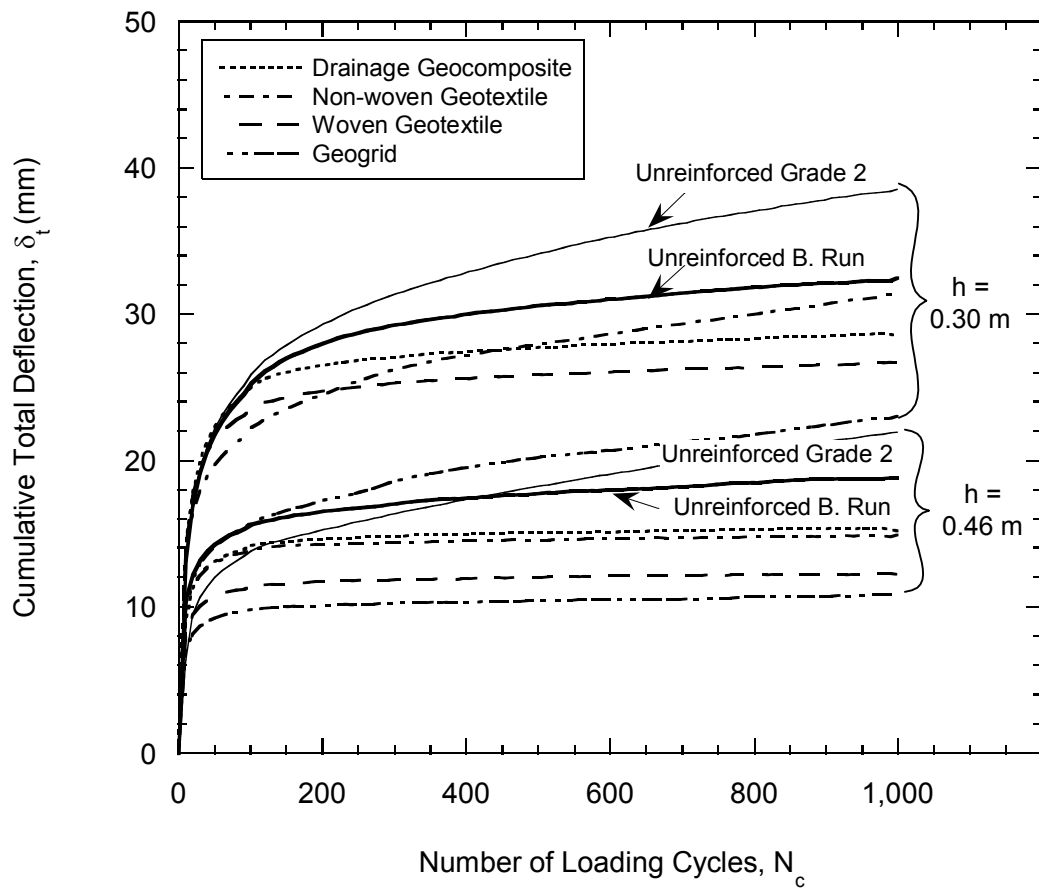


Fig. 2. 5. Cumulative total deflection ( $\delta_t$ ) under the loading plate of the LSME as a function of number of load cycles for aggregate platforms having a thickness ( $h$ ) of 0.30 m or 0.46 m. Geosynthetic-reinforced platforms are constructed only with Grade 2.

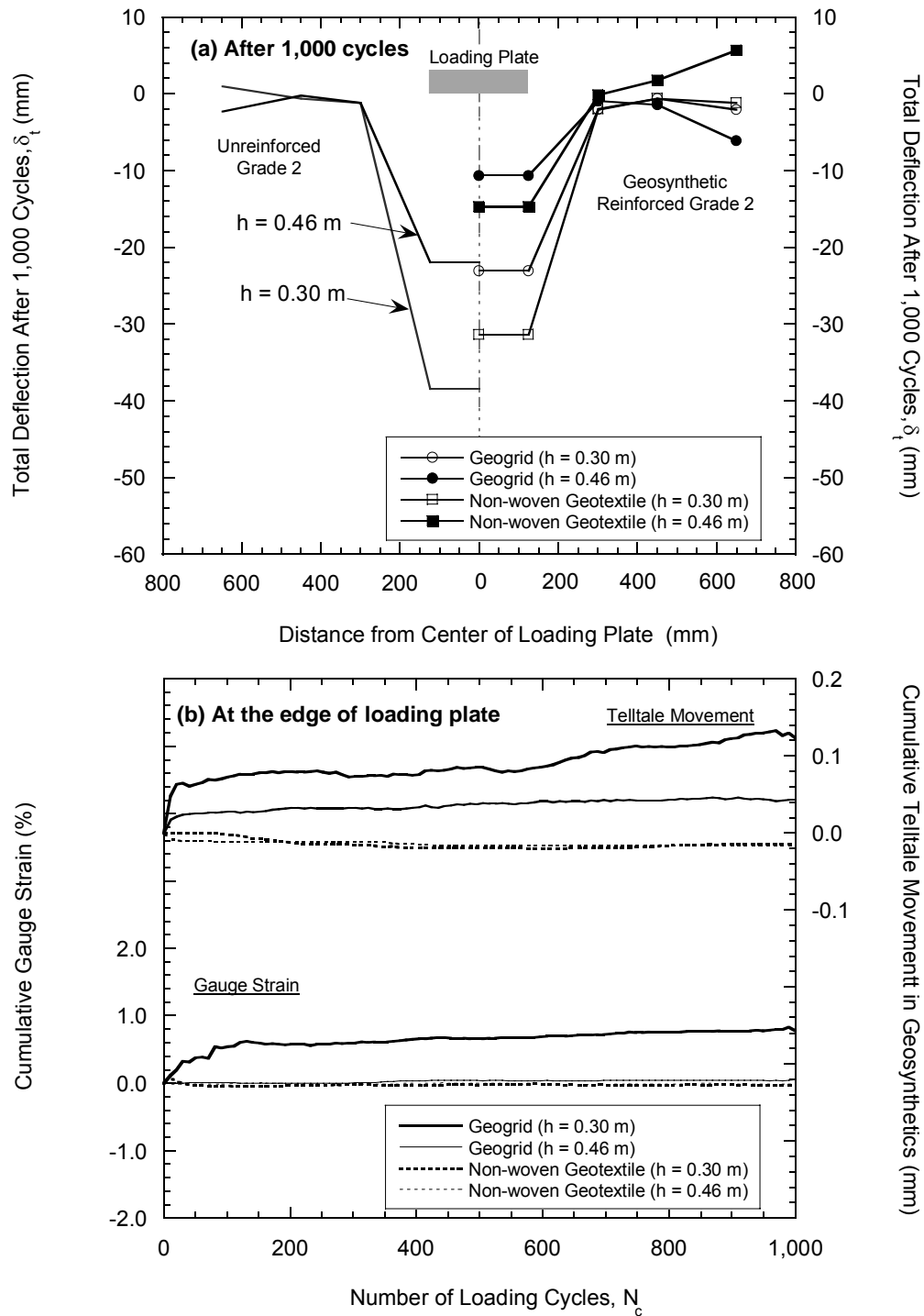


Fig. 2.6. Effect of layer thickness on the total deflection for geogrid and non-woven geotextile-reinforced platforms in the LSME: (a) deflection basins after 1,000 load cycles and (b) gauge strain and telltale movement in the geosynthetic at the edge of the loading plate as a function of number of load cycles.

by making the platform thicker is higher for the geogrid- and the non-woven geotextile-reinforced platforms (i.e., 53%) than that for the unreinforced aggregate platform (i.e., 43%). For the platform reinforced with less extensible geosynthetic material (i.e., requiring smaller relative movement to develop interaction with the aggregate) such as geogrid in this study, the layer thickness effect on the total deflection can be demonstrated by measuring the gauge strain and the telltale movement in the geosynthetic at the edge of loading plate, as shown in Fig. 2.6b. The thicker the geogrid-reinforced platform layer is, the less strain and the telltale movement are measured during the loading cycles. However, this tendency is not evident for the more extensible geosynthetic material such as non-woven geotextile in this study because of the difference in polymers, stress-strain behavior, and interaction between the geosynthetic and the aggregate platform material. A more detailed discussion is given in the subsequent section.

### **2.6.2.3 Effect of Geosynthetic Type on The Total Deflection Basins**

The effect of reinforcing geosynthetic type on the total deflection basin at 1,000 cycles is illustrated in Fig. 2.7a for Grade 2 platforms reinforced with geosynthetics. The reinforced working platform is 0.30-m thick in each case. Deflections under the loading plate are approximately 18%, 26%, 31%, and 40% smaller for the non-woven geotextile, drainage geocomposite, woven geotextile, and geogrid, respectively, than that for the unreinforced Grade 2 only. Although less deflection are obtained from geosynthetic-reinforced Grade 2 working platforms,

their load-deflection behaviors are differentiated. The cumulative gauge strain and telltale movement in the geosynthetic at the edge of the loading plate during 1,000 load cycles are shown in Fig. 2.7b. LSME test with geogrid as a platform reinforcement shows the largest telltale downward movement and the second largest accumulative gauge strain (= 0.8%) at the edge of the loading plate among all geosynthetics, while the largest cumulative gauge strain (= 1.5%) and nearly nil telltale movement are measured in the woven geotextile. Almost no strains and telltale movements are measured in the non-woven geotextile and the drainage geocomposite for the load cycles in the LSME tests.

To explain the observed responses of the geosynthetic in the aggregate platform, a direct comparison between the tensile strengths measured from the wide width test (Fig. 2.2) and those measured in the LSME tests cannot be made because of the difference in testing method (i.e., index test versus performance test). In the performance test such as LSME in this study with the geogrid, the interlocking between aggregate and geogrid and the stiffness of the geogrid are probably the factors responsible for this type of response. On the other hand, the interface friction between the aggregate and the non-woven geotextile or drainage geocomposite may play a major role in the LSME and seems to be developed at a lesser downward movement than with the geogrid. However, a relative comparison of the load and deflection behavior can be made by comparing the hierarchy of the moduli (offset tangent and secant moduli) from the wide width tensile test, the interaction modulus from the pullout test (Fig. 2.8), and the deflection after 1,000 load cycles in the LSME for each geosynthetic (Fig. 2.7). Both the measured

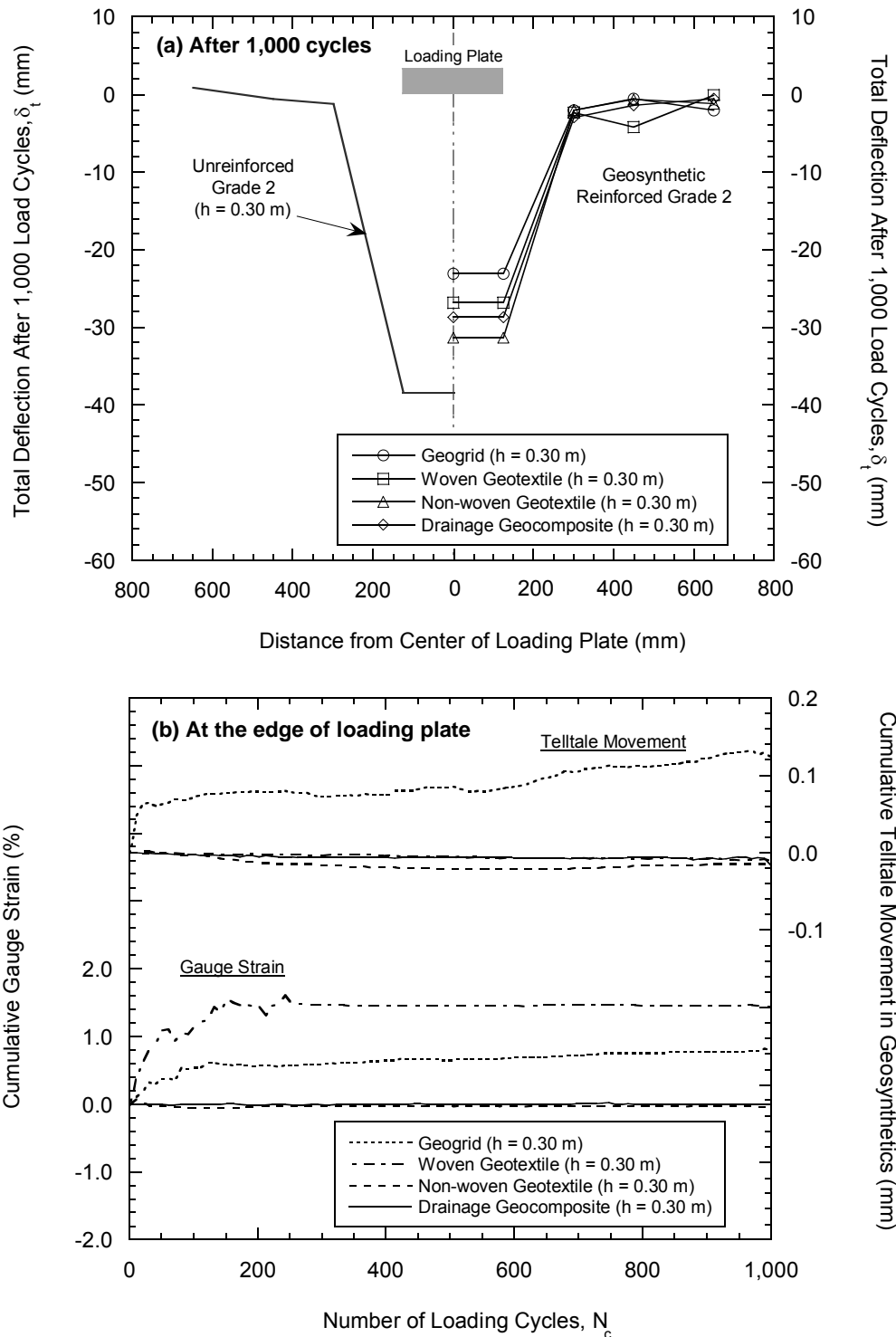


Fig. 2.7. Effect of geosynthetic type on the total deflection for Grade 2 platforms reinforced with geosynthetics when the platform thickness is 0.30 m (i.e.,  $h = 0.30$  m): (a) deflection basins after 1,000 load cycles in the LSME and (b) gauge strain and telltale movement in the geosynthetic at the edge of the loading plate as a function of number of load cycles.

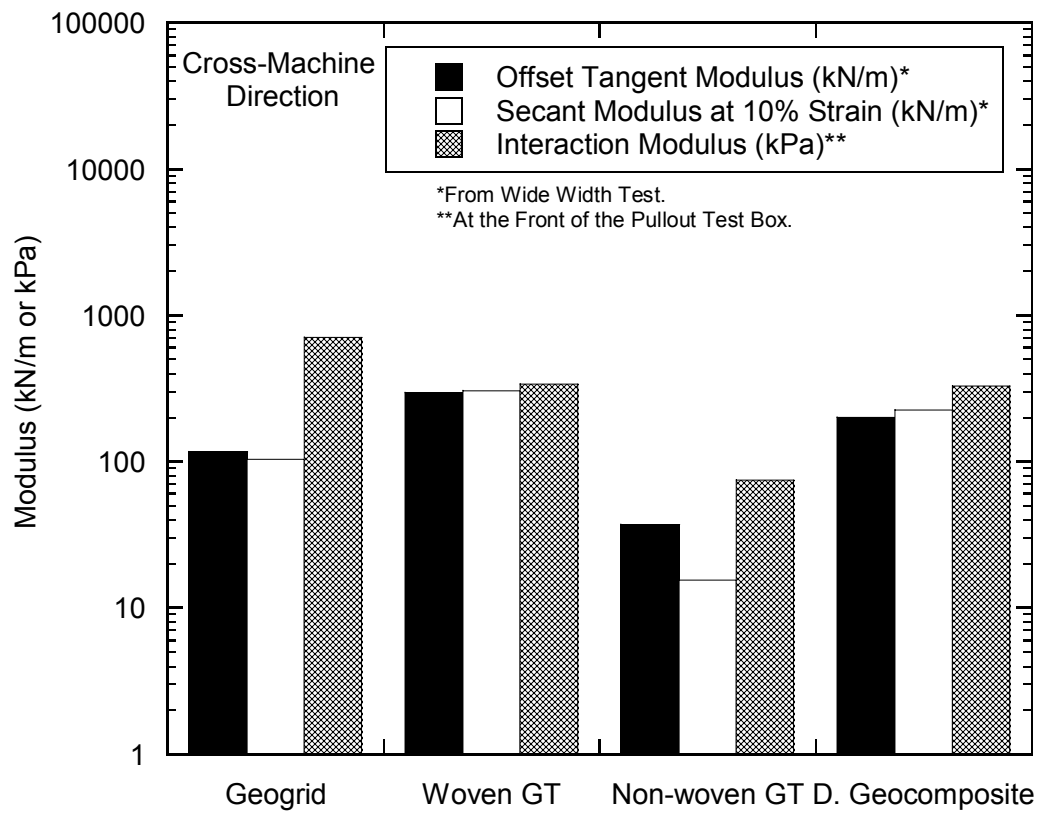


Fig. 2.8. Comparison of moduli in the cross machine direction from wide width tensile test and the pullout test for geosynthetics used in the LSME.

deflections in the LSME tests and the interaction modulus from the pullout tests fall in the same order, with the smallest deflection (i.e., 23 mm) and the largest interaction modulus (i.e., 699kPa) in the cross-machine direction, i.e., a much higher engagement, associated with the geogrid and the largest deflection and smallest interaction modulus associated with the non-woven geotextile (i.e., 31 mm of deflection and 74 kPa of interaction modulus). However, index moduli of the geosynthetics as obtained from the wide-width tensile tests do not correlate with the deflections observed after 1,000 load cycles in the LSME.

The deflection basins in Fig. 2.6a and Fig. 2.7a also show the relative stiffness of each geosynthetic reinforced aggregate platform. For the reinforced Grade 2 platforms of equal layer thickness, deflections under the loading plate are smaller for the geogrid than for the non-woven geotextile. However, an aggregate working platform can be reinforced with the non-woven geotextile (or another alternative geosynthetic) that is equivalent to a geogrid reinforced working platform in terms of total deflection by using a thicker layer. Furthermore, the deflection basins also show the region of influence of the loading plate. The total deflection diminishes rapidly with distance, and is very small (< 5 mm) for all materials at a distance of 300 mm from the center of the loading plate (175 mm from the edge of the loading plate). Therefore, all subsequent comparisons are based on deflections directly under the loading plate.

### 2.6.3 Permanent Deformation Analysis

Permanent deformation of the working platform in pavement systems can be one of the significant design criteria because of causing rutting of the platform surface and impacting construction and asphalt placement. Thus, permanent deformation is required not exceed a regulatory maximum. To predict the rate of rutting in a working platform based on the deformation response during cyclic loading in the LSME, a rutting curve, defined as a log-log plot of cumulative permanent strain (i.e., plastic strain obtained by subtracting elastic strain from total strain) as a function of the number of applied loads is plotted for each aggregate platform testing. The rutting curves for the 0.30-m thick Grade 2 platforms reinforced with geogrid and drainage geocomposite and without reinforcement are shown in Fig. 2.9 as illustrative examples; rutting curves similar in shape to that of the drainage geocomposite were obtained for woven and non-woven geotextile reinforcements. A straight line was fitted to the linear portion of the rutting curve with a slope (S) and intercept (I). . The linear portion of the rutting curve is defined in this study as the loading cycle where the rate of change of the permanent strain does not change with the subsequent load cycles. Strain rates were determined by fitting a power function to the data. The rutting characteristics for the working platforms in the LSME are summarized in Table 2.3 in terms of S and I of the linear portion of the rutting curves using the VESYS method as discussed by Huang (1993). The parameter S is the rate of increase of non-recoverable strain as a function of the number of stress repetitions, and the parameter I is the initial offset, considered to be due to initial densification of the pavement structure layer due to

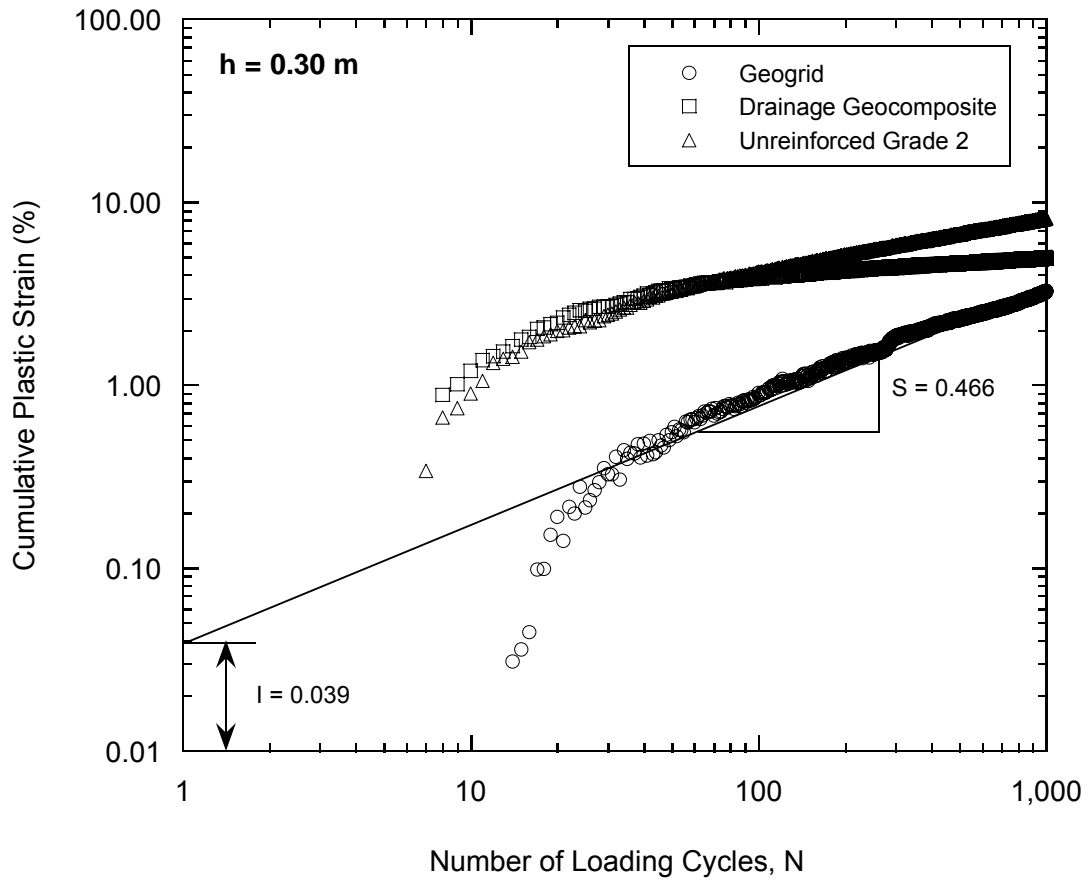


Fig. 2.9. Accumulation of plastic strain during the LSME test of Grade 2 with and without geosynthetic reinforcement ( $h$  = working platform thickness).

Table 2.3. Permanent Deformation Parameters With and Without Geosynthetic Reinforcements.

| Geosynthetic Reinforcement | Platform Thickness (m) | I                    | S      | $\epsilon_p$ at N = 1000 |
|----------------------------|------------------------|----------------------|--------|--------------------------|
| None (Grade 2)             | 0.30                   | $7.8 \times 10^{-3}$ | 0.2745 | $8.1 \times 10^{-2}$     |
|                            | 0.46                   | $1.3 \times 10^{-3}$ | 0.4599 | $2.8 \times 10^{-2}$     |
| None (Breaker Run)         | 0.30                   | $1.0 \times 10^{-2}$ | 0.2741 | $6.3 \times 10^{-2}$     |
|                            | 0.46                   | $4.8 \times 10^{-3}$ | 0.1682 | $1.9 \times 10^{-2}$     |
| Geogrid                    | 0.30                   | $3.9 \times 10^{-3}$ | 0.4660 | $3.3 \times 10^{-2}$     |
|                            | 0.46                   | $3.0 \times 10^{-3}$ | 0.1654 | $7.6 \times 10^{-3}$     |
| Woven Geotextile           | 0.30                   | $1.6 \times 10^{-2}$ | 0.0969 | $4.3 \times 10^{-2}$     |
|                            | 0.46                   | $5.1 \times 10^{-3}$ | 0.0742 | $9.5 \times 10^{-3}$     |
| Non-woven Geotextile       | 0.30                   | $7.6 \times 10^{-3}$ | 0.3243 | $6.0 \times 10^{-2}$     |
|                            | 0.46                   | $8.4 \times 10^{-3}$ | 0.0637 | $1.4 \times 10^{-2}$     |
| Drainage Geocomposite      | 0.30                   | $1.7 \times 10^{-2}$ | 0.0980 | $4.9 \times 10^{-2}$     |
|                            | 0.46                   | $2.6 \times 10^{-3}$ | 0.1104 | $9.2 \times 10^{-3}$     |

construction and the first passes of traffic (Mengelt et al. 2000). In general, softer materials will have higher intercepts and slopes, indicating that rutting will occur at a faster rate than in stiffer materials.

For the 0.30-m thick working platforms, the higher initial offset ( $= 1.7 \times 10^{-2}$ ) and the lower rate of cumulative plastic strain ( $= 0.098$ ) are obtained in the drainage geocomposite-reinforced platform, while the lower initial offset ( $= 3.9 \times 10^{-3}$ ) and the higher rate of strain ( $= 0.466$ ) are obtained in the geogrid-reinforced platform. The parameters I and S for both woven and non-woven geotextile-reinforced platforms range between the values for the geogrid and the drainage geocomposite. For the thicker ( $= 0.46$  m) platform layers, the differences in the parameters I and S for the geogrid and the drainage geocomposite diminished. As the working platform becomes thicker, the values of initial offset for all the testing platforms in the LSME decrease and fall in the same order of magnitude. The initial offset, I, is slightly lower for the unreinforced Grade 2 working platform than that for the reinforced platforms. On the other hand, the working platforms reinforced by geosynthetics tend to accumulate permanent strain at a significantly slower rate than in the unreinforced platform. As a result, less rutting will occur in the reinforced platforms even though the initial offset is slightly higher.

#### **2.6.4 Relationship Between Platform Thickness and Total Deflection**

Defining equivalent geosynthetic-reinforced aggregate platforms requires a functional relationship between the working platform thickness ( $h$ ) and total

deflection ( $\delta_t$ ) at 1,000 cycles obtained from the LSME for each reinforcing geosynthetic. The total deflections associated with the platform thickness under the loading plate of the LSME for the geosynthetic-reinforced Grade 2 platforms are compared with that for the unreinforced breaker run after 1,000 load cycles. These  $h$ - $\delta_t$  relationships can be used to identify the thickness of a geosynthetic-reinforced aggregate platform that provides the same deflection as a working platform of breaker run. Geosynthetic-reinforced aggregate platform thickness required to achieve the total deflection limited to 12.5 mm, 25.0 mm, and 37.5 mm (depending on the designer's choice) are summarized in Table 2.4. For example, a 0.31-m-thick platform of woven geotextile reinforced Grade 2 generates the same total deflection (25 mm under the loading plate) as a 0.36-m-thick working platform of the unreinforced breaker run and a 0.41-m-thick platform of the unreinforced Grade 2. Because only two different layers (i.e., 0.30-m and 0.46-m thick) of the geosynthetics-reinforced platforms are tested in the LSME, the deflections at 1,000 cycles beyond those thicknesses were extrapolated linearly from the deflections measured for two layers.

Based on the total deflections limited to 12.5 mm, 25.0 mm, and 37.5 mm, the normalized platform thickness ratios between the unreinforced breaker run and the unreinforced and geosynthetic-reinforced Grade 2 platforms tested in the LSME under the same load at 1,000 cycles, are compared in Fig. 2.10. Breaker run thickness is used in normalizing because it is the traditional working platform material with which there is considerable experience. A slightly thicker (10 to 20%)

aggregate platform is required when unreinforced Grade 2 is used instead of breaker run. However, when the Grade 2 working platform constructed over the soft subgrades is reinforced with geosynthetics, thinner working platforms than breaker run are required. The least normalized equivalent thickness is obtained by

Table 2.4. Geosynthetic-Reinforced Aggregate Platform Thickness (h in meters) Required to Achieve the Total Deflection ( $\delta_t$  in millimeters) Limited to 12.5 mm, 25.0 mm, and 37.5 mm

| Geosynthetic Reinforcement | Total Deflection ( $\delta_t$ ) |         |         |
|----------------------------|---------------------------------|---------|---------|
|                            | 12.5 mm                         | 25.0 mm | 37.5 mm |
| None (Breaker Run)         | 0.63 m                          | 0.36 m  | 0.27 m  |
| None (Grade 2)             | 0.69 m                          | 0.41 m  | 0.31 m  |
| Geogrid                    | 0.42 m                          | 0.28 m  | 0.22 m  |
| Woven Geotextile           | 0.45 m                          | 0.31 m  | 0.25 m  |
| Non-woven Geotextile       | 0.51 m                          | 0.35 m  | 0.27 m  |
| Drainage Geocomposite      | 0.53 m                          | 0.33 m  | 0.25 m  |

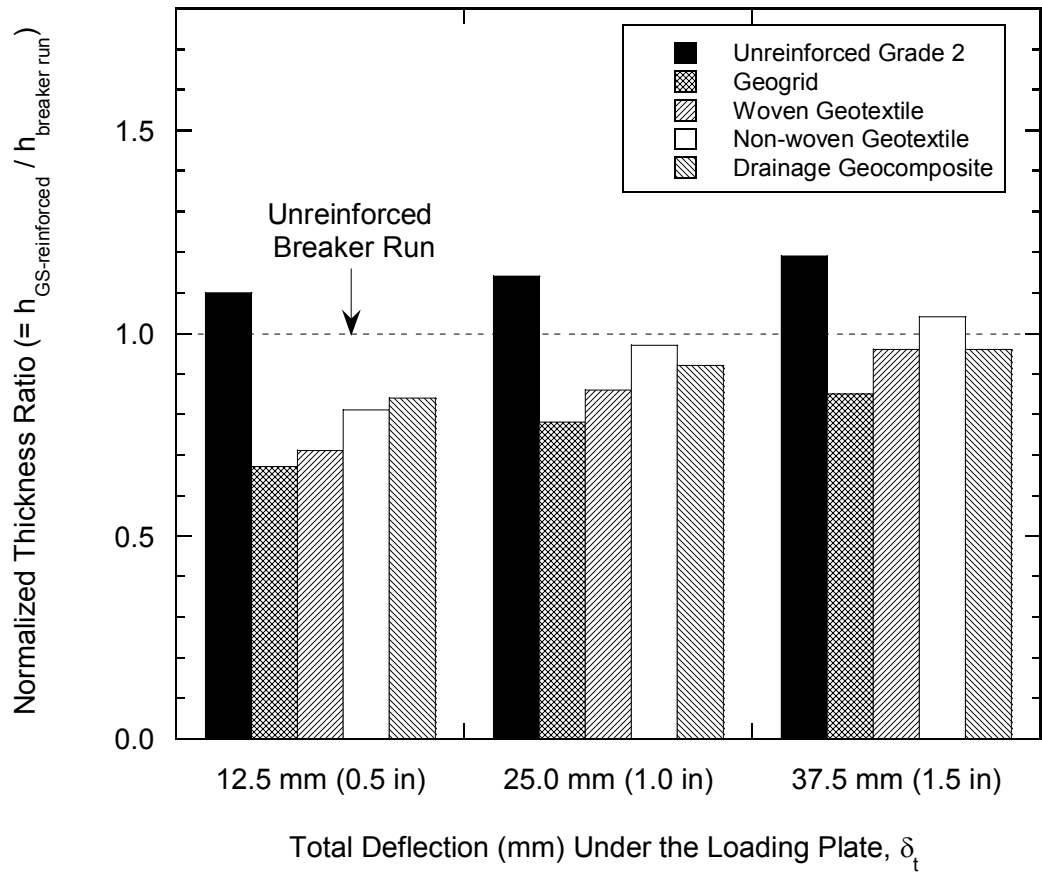


Fig. 2.10. Comparison of normalized equivalency thickness between the unreinforced breaker run and the geosynthetic-reinforced Grade 2 tested based on the total deflections limited to 12.5, 25.0, and 37.5 millimeters.

the geogrid reinforcement. The reduction in the platform layer thickness by the geosynthetic reinforcements for 25.0 mm total deflection ranges from 3% to 22% of the unreinforced breaker run thickness. The benefit of reinforcement is partially reduced because of the higher stiffness of breaker run compared to Grade 2. In addition, the effect of the geosynthetic reinforcement on the reduction of the working platform thickness is particularly noticeable when a smaller total deflection is required. Note that the relationships shown in Fig. 10 are based on the LSME test models for the specific geosynthetic used in this study and for a very soft subgrade condition with the simulated subgrade CBR assumed to be one.

### **2.6.5 Equivalency Chart**

The normalized thickness ratio determined from the relationship between the platform thickness and total deflection for each test material now can be used to determine the equivalent thickness for alternative geosynthetic-reinforced aggregate platforms. Equivalency, as defined here, requires that the total deflection of the alternative geosynthetic-reinforced platform is equal to that of the breaker run platform under the same load at 1,000 cycles. The equivalent thickness for geosynthetic-reinforced platforms can be determined by multiplying the thickness of the breaker run corresponding to a chosen total deflection by the normalized thickness ratio for that total deflection. The equivalency chart (Fig. 2.11) is developed to aid in selecting the thickness of an alternative geosynthetic-reinforced

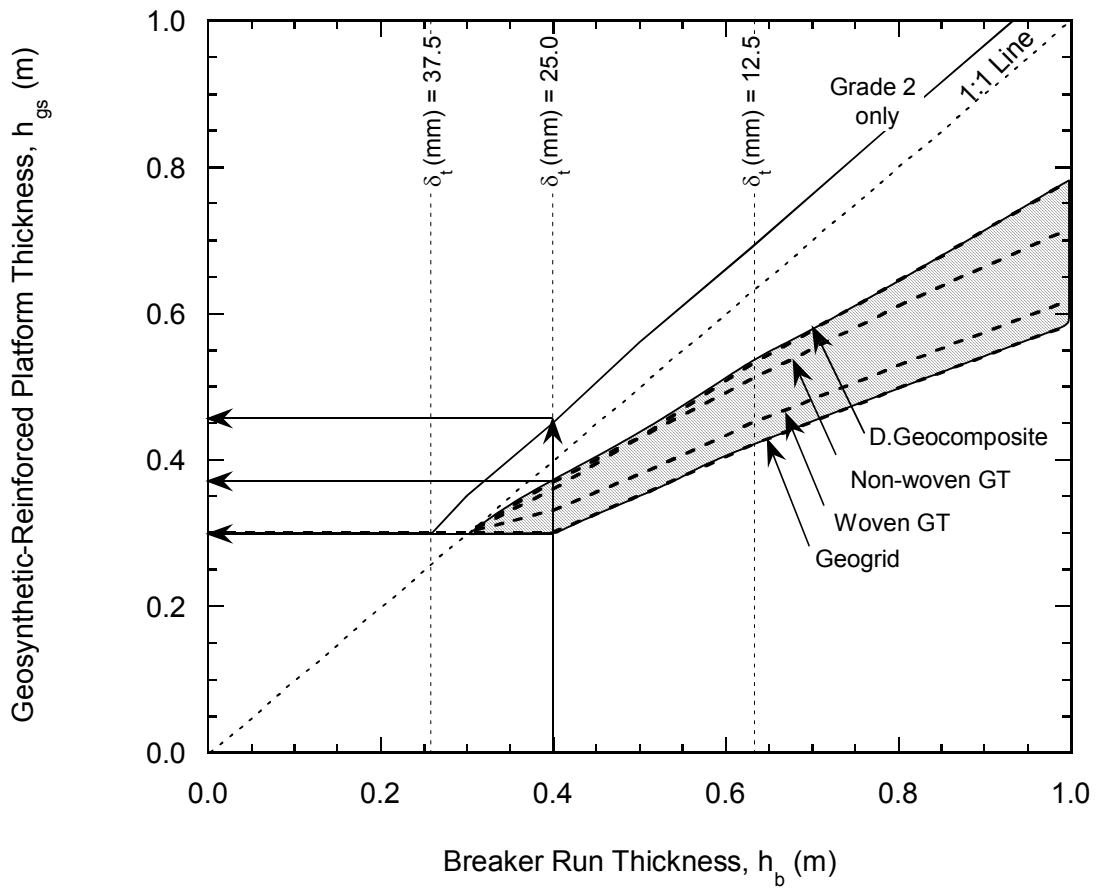


Fig. 2.11. Equivalency chart relating thickness of each geosynthetic-reinforced platform to the thickness of the breaker run.

aggregate platform that will provide a working platform performance equivalent to that of a layer of breaker run.

To determine the minimum layer thickness of the aggregate platforms constructed over soft subgrades, the unpaved road design method described in Giroud and Noiray (1981) was used to make a direct comparison between the working platform thickness ( $h$ ) and the aggregate layer thickness (Tanyu et al., 2004). The acceptable total deflection was assumed to be 38 mm, which is a typical criterion for working platforms in the Midwestern US. According to Tanyu et al. (2004), Giroud and Noiray's method requires an unreinforced aggregate thickness of 0.30 m to limit total deflections to 38 mm, whereas Table 2.4 requires an aggregate platform with a thickness of 0.27 m if built by breaker run or 0.31 m if built by Grade 2. There is a negligible difference in thickness between the Giroud and Noiray's method and the experimental results of this investigation. Therefore, as shown in Fig. 2.10, 0.30-m-thick layer of breaker run and alternative reinforced aggregate platforms are assumed to be the minimum working platform thickness over the very soft subgrades in this study. Furthermore, from a practical point of view, this thickness is probably the minimum reasonable thickness for working platform with breaker run, which consists mostly of cobbles and gravel. For a 0.4-m-thick working platform of breaker run, equivalent reinforced platforms can be constructed with 0.30 m of geogrid-, 0.33 m of woven geotextile-, 0.37 m of non-woven geotextile-, 0.36 m of drainage geocomposite-reinforced Grade 2, or 0.45 m of unreinforced Grade 2. The equivalency chart shown in Fig. 2.11 applies only to the geosynthetic materials tested in this study. Site-specific criteria such as type of highway and whether the

working platform will be included in the pavement structural design as subbase should also be considered when designing working platforms reinforced with geosynthetics. However, this methodology can be used in other reinforcement-aggregate platforms.

## 2.7 PRACTICAL IMPLICATIONS

The chart shown in Fig. 2.11 is conceptual and applies directly only to the geosynthetic-reinforced materials tested in this study. One approach to generalize the equivalency method is to relate the total deflections to readily measurable properties of geosynthetic-reinforced working platform materials, such as the interaction modulus from a pullout test. Such a chart is shown in Fig. 2.12, which relates the ratio  $h_{gs}/h_b$  determined from the LSME test to the interaction modulus obtained from the pullout test for platform total deflections of  $\delta_t = 25$  mm and 50 mm. Linear lines are fitted for these total deflections ( $\delta_t$ ), which are considered to be the acceptable total deflections for working platforms in the Midwestern US based on a study of subgrade deflection criteria by Croveti and Schabelski (2001). The relationships shown in Fig. 2.12 can be used for selecting the alternative thickness of a geosynthetic-reinforced material that will provide a working platform equivalent to a layer of traditionally used breaker run.

The following example explains how the design chart is used. Assume that the original design calls for a 0.4-m-thick working platform of breaker run. For a geosynthetic with a given interaction modulus ( $M_i$ ) from the pullout test, thicknesses

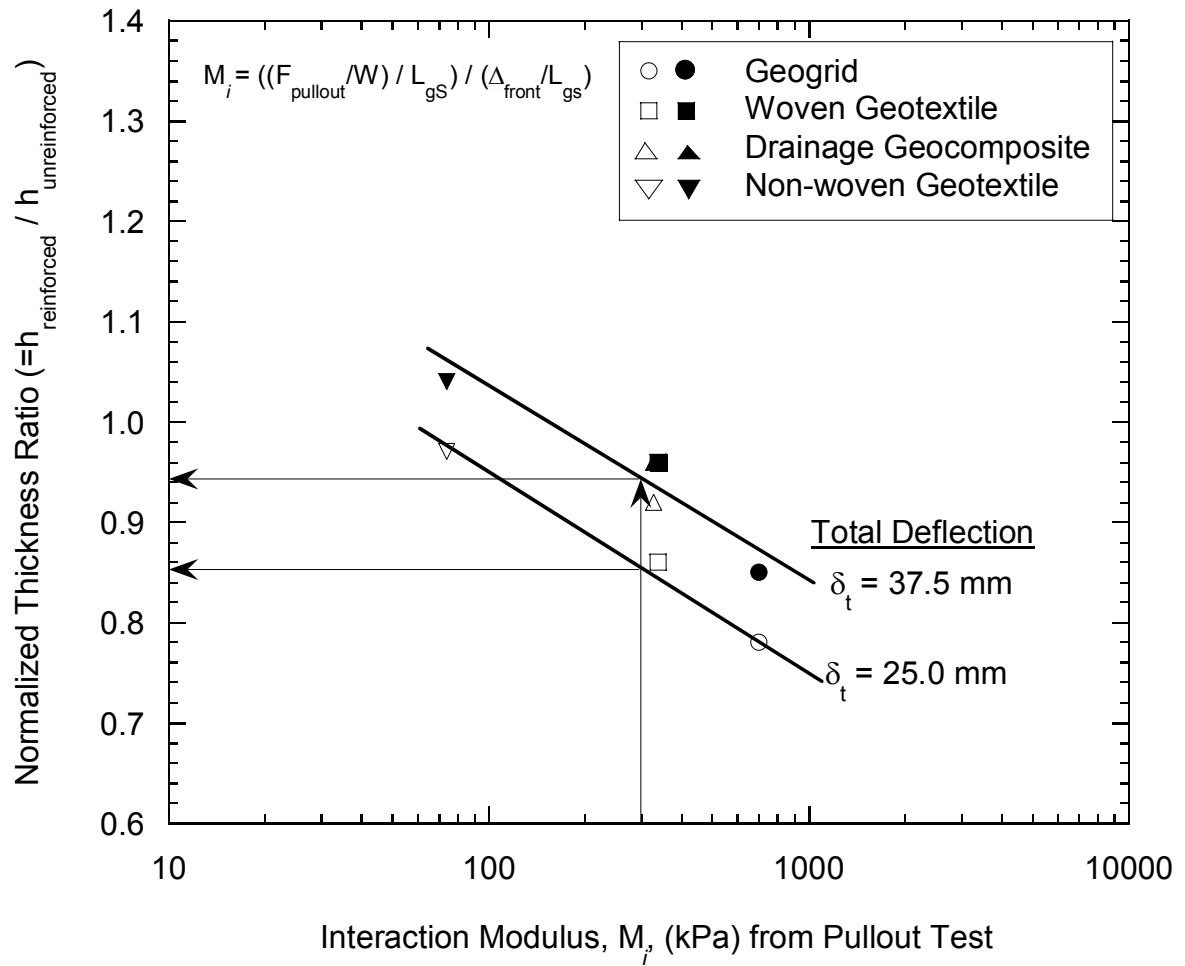


Fig. 2.12. Relationship between the normalized equivalency thicknesses and the interaction modulus from the pullout test for various geosynthetics.

of an alternative geosynthetic-reinforced material is then identified by extending a vertical line from the abscissa to each line on the graph. For  $h_b = 0.4$  m and  $M_i = 300$  kPa, an equivalent geosynthetic-reinforced working platform can be constructed with either a thickness of 0.34 m or 0.38 m corresponding respectively to the acceptable total deflections of  $\delta_t = 25.0$  mm or 37.5 mm. Designers should keep in mind the nature of this chart when applying the equivalency approach and not extrapolate to much different conditions. Site-specific criteria (e.g., type of highway, whether the working platform will be included in the pavement structural design as subbase, availability of materials, final elevations and required cut depth, etc.) should also be considered when designing working platforms reinforced with geosynthetics.

## **2.8 CONSTRUCTION ISSUES**

The construction of alternative material sections in the field are described in another report (WHRP Project SPR #0092-45-98). The geosynthetics (woven and nonwoven geotextiles, geogrid, and geocomposite drainage layer) were placed using a similar procedure. The geosynthetic layer spread over the prepared subgrade and excavated rock was placed over the layer using a loader in a single lift. Spreading the geocomposite drainage layer, which was delivered to the site as pre-assembled panels wide enough to cover each lane required greater effort than the other geosynthetics, but was accomplished without the use of any heavy

equipment. The field test sections were monitored at different intensity for 5 years. Further details of construction and performance of field sites based on the monitoring data collected can be found in WHRP Project SPR #0092-45-98 report.

## **2.9 SUMMARY AND CONCLUSIONS**

Large-scale model experiments (LSME) were conducted on each of the geosynthetic-reinforced aggregate working platforms to define the relationship between total deflection and working platform thickness for a typical construction loading. The effects of the reinforced platform thickness and the type of geosynthetics on the total deflection were evaluated. In addition, the permanent deformation analysis using VESYS model was conducted to predict the rate of rutting in a working platform based on the deformation response during cycle loading in the LSME. A geosynthetic-reinforced working platform was considered equivalent if the total deflection of the reinforced material was equal to that of breaker run under the same construction loading. Results of LSME tests were used to develop equivalency chart relating the thickness of an alternative material with geosynthetic reinforcement required to achieve the same total deflection as a working platform of breaker run.

Based on the LSME test results, the total deflections were reduced by 18% to 40% for the 0.30-m thick and by 31% to 51% for the 0.46-m-thick geosynthetic-reinforced platforms compared to the unreinforced Grade 2 platform. Also, the smaller total deflections were observed for the thicker layer (0.46 m) of reinforced

platforms. The reduction rate in the total deflection by making the platform thicker is higher for the geogrid- and the non-woven geotextile-reinforced platforms than that for the unreinforced aggregate platform. The working platforms reinforced by geosynthetics tend to accumulate permanent strain at a significantly slower rate than in the unreinforced platform, resulting in less rutting. The equivalency chart shows that the effect of the geosynthetic reinforcement on the reduction of the working platform thickness is particularly noticeable when a smaller total deflection is required. The relationships in the equivalency chart are based on the LSME tests for the specific geosynthetics used in this study and for a very soft subgrade condition with the simulated subgrade CBR assumed to be one. Therefore, site-specific criteria such as type of highway and whether the working platform will be included in the pavement structural design as subbase should also be considered when designing working platforms reinforced with geosynthetics. However, this methodology can be used in other reinforcement-aggregate platforms.

### **3.0 REFERENCES**

- AASHTO, 1994, "Standard Method of Test for Resilient Modulus of Unbound Granular Base/Subbase Materials and Subgrade Soils," T 294, Protocol P46, American Association of State Highway and Transportation Officials, pp. 794-807.
- Chew, S. H., Wong, W. K., Ng, C. C., Tan, S. A., and Karunaratne, G. P., 2000, "Strain Gauging Geotextiles Using External Gauge Attachment Method," Grips, Clamps, Clamping Techniques, and Strain Measurement for Testing of Geosynthetics, ASTM STP 1379, P.E. Stevenson, Eds., ASTM, West Conshohocken, PA, pp. 97-110.

- Chou, Y. T., 1976, "Analysis of Subgrade Rutting in Flexible Airfield Pavements," Transportation Research Record 616, Transportation Research Board, National Research Council, Washington, DC, pp. 44-48.
- Christopher, B. R., and Holtz, R. D., 1985, "Geotextile Engineering Manual," Report No. FHWA-TS-86/203, U.S. Department of Transportation, Federal highway Administration, Washington, DC, March, p. 1044.
- Crovetti, J. A., and Schabelski, J. P., 2001, Comprehensive Subgrade Deflection Acceptance Criteria, Phase III Final Report WI/SPR 02-01, WisDOT, Highway Research Study #98-1, SPR #0092-45-95.
- Fannin, R. J., and Sigurdsson, O., 1996, "Field Observations on Stabilization of Unpaved Roads with Geosynthetics," Journal of Geotechnical Engineering, ASCE, Vo. 122, No. 7, pp. 544-553.
- Farrag K., 1999, "Strain Gage Installation on Geosynthetics," Louisiana Transportation Research Center, Louisiana State University, Baton Rouge, LA.
- Finn, F., Saraf, C. L., Kulkarni, R., Nair, K., Smith, W., and Abdullah, A., 1986, "Development of Pavement Structural Subsystems," NCHRP Report 291, Transportation Research Board, National Research Council, Washington, DC.
- Giroud, J. P., and Noiray, L., 1981, "Geotextile Reinforced Unpaved Road Design," Journal of Geotechnical Engineering Division, ASCE, Vol. 107, No. GT9, pp. 1233-1254.
- Giroud, J. P., Ah-Line, C., and Bonaparte, R, 1984, "Design of Unpaved Roads and Trafficked Areas with Geogrids," Polymer Grid Reinforcement: A Conference Sponsored by SERC and Netlon, Ltd., Thomas Telford, London, England, pp. 116-127.
- Goodhue, M. J., Edil, T. B., and Benson, C. H., 2001, "Interaction of Foundry Sands with Geosynthetics," Journal of Geotechnical and Geoenvironmental Engineering, ASCE, Vol. 127, No. 4, pp. 353-362.
- Hayden, S. A., Humphrey, D. N., Christopher, B. R., Henry, K. S., and Fetten, C. P., 1999, "Effectiveness of Geosynthetics for Roadway Construction in Cold Regions: Results of a Multi-Use Test Section," Proceedings of Geosynthetics '99, Vol. 2, Boston, MA, pp. 847-862.
- Holtz, R. D., Christopher, B. R., and Berg, R. R., 1995, "Geosynthetic Design and Construction Guidelines," Report No. FHWA-HI-95, U.S. Department of Transportation, Federal Highway Administration, National Highway Institute Course No. 13213, Washington, DC.

- Huang, Y. H., 1993, *Pavement Analysis and Design*, Prentice Hall, Englewood Cliffs, New Jersey.
- Huntington, G., and Ksaibati, K., 2000, "Evaluation of Geogrid-reinforced Granular Base," *Geotechnical Fabrics Report*, January/February, pp. 22-28.
- Koerner, R. M., 1998, *Designing With Geosynthetics*, Fourth Edition, Prentice Hall, Englewood Cliffs, New Jersey.
- Leng, J., and Garb, M. A., 2002, "Characteristics of Geogrid-Reinforced Aggregate Under Cyclic Load," *Transportation Research Record 1786*, Transportation Research Board, National Research Council, Washington, DC, pp. 29-35.
- Li, D., and Selig, T., 1996, "Cumulative Plastic Deformation for Fine-Grained Subgrade Soils," *Journal of Geotechnical Engineering*, ASCE, Vol. 122, No.12, pp. 1006-1013.
- Mengelt, M. J., Edil, T. B., and Benson, C. H., 2000, "Reinforcement of Flexible Pavements Using Geocells," *Geotechnical Engineering Report 00-04*, Department of Civil and Environmental Engineering, University of Wisconsin-Madison, Madison, Wisconsin, p. 180.
- Madhav, M. R., Gurung, N., and Iwao, Y., 1998, "A Theoretical Model for the Pullout Response of Geosynthetic Reinforcement," *Geosynthetics International*, Vol. 5, No. 4, pp. 399-427.
- Miura, N., Sakai, A., Taesiri, Y., Yamanouchi, T. and Yasuhara, K., 1990, "Polymer Grid Reinforced Pavement on Soft Clay Grounds," *Geotextiles and Geomembranes*, Vol. 9, No. 1, pp. 99-123.
- Monismith, C. L., Ogawa, N., and Freeme, C. R., 1975, "Permanent Deformation Characteristics of Subgrade Soils Due to Repeated Loading," *Transportation Research Record 537*, Transportation Research Board, National Research Council, Washington, DC, pp. 1-17.
- Montanelli, F., Zhao, A., and Rimoldi, P., 1997, "Geosynthetic-Reinforced Pavement System: Testing and Design," *Proceedings of Geosynthetics '97*, IFAI, Vol. 2, Long Beach, California, pp. 619-632.
- Mudrey, M. G., Brown, B. A., and Greenberg, J. K., 1982, *Bedrock Geologic Map of Wisconsin*, Geological and Natural History Survey, University of Wisconsin-Extension.

- Negussey, D., and Jahanandish, M., 1993, "Comparison of Some Engineering Properties of Expanded Polystyrene with Those of Soils," *Transportation Research Record 1418*, Transportation Research Board, National Research Council, Washington, DC, pp. 43-50.
- Perkins, S. W., 1999, "Mechanical Response of Geosynthetic-Reinforced Flexible Pavements," *Geosynthetics International*, Vol. 6, No. 5, pp. 347-382.
- Perkins, S. W. and Cuelho, E. V., 1999, "Soil-Geosynthetic Interface Strength and Stiffness Relationships from Pullout Tests," *Geosynthetics International*, Vol. 6, No. 5, pp. 321-346.
- Tanyu, B. F., Kim, W. H., Edil, T. B., and Benson, C. H., 2003, "Comparison of Laboratory Resilient Modulus with Back-Calculated Elastic Moduli from Large-Scale Model Experiments and FWD Tests on Granular Materials," *Resilient Modulus Testing for Pavement Components*, ASTM STP 1437, Paper ID 10911, G. N. Durham, A. W. Marr, and W. L. De Groff, Eds., ASTM International, West Conshohocken, PA, 191-208.
- Tanyu, B. F., Benson, C. H., Edil, T. B., and Kim, W. H., 2004, "Equivalency of Crushed Rock and Three Industrial By-products Used for Working Platforms During Pavement Construction," *Transportation Research Record*, Paper No. 04-3105, Transportation Research Board, Washington, DC, (in press).
- Tatliso, N., Edil, T. B., and Benson, C. H. 1998, "Interaction Between Reinforcing Geosynthetics and Soil-tire Chip Mixtures," *Journal of Geotechnical and Geoenvironmental Engineering*, ASCE, 124 (11), 1109-1119.
- Thompson, M. R., and Nauman, D., 1993, "Rutting Rate Analyses of the ASSHTO Road Test Flexible Pavements," *Transportation Research Record 1384*, Transportation Research Board, National Research Council, Washington, DC, pp. 36-48.
- WisDOT, 1996, *Standard Specifications for Highway and Structure Construction*, Wisconsin Department of Transportation, Madison, Wisconsin. p. 754.
- WisDOT, 1997, *Subgrade Design/Construction Process Review*, District 1 Final Report, State of Wisconsin, Department of Transportation.
- WisDOT, 2003, *Facilities Development Manual*, State of Wisconsin, Department of Transportation.
- Zhao, A., and Foxworthy, P. T., 1999, "Geogrid Reinforcement of Flexible Pavements: a Practical Perspective," *Geotechnical Fabrics Report*, may, pp. 28-34.

Zou, Y., Small, J. C., and Leo, C. J., 2000, "Behavior of EPS Geofoam as Flexible Pavement Subgrade Material in Model Tests," *Geosynthetics International*, Vol. 7, pp. 1-22.